FULL PAPER

Synthesis of nitro-aryl functionalised 4-amino-1,8-naphthalimides and their evaluation as fluorescent hypoxia sensors

Liam D. Adair[a], Natalie Trinh[a], Pauline M. Vérité[b], Denis Jacquemin[b], Katrina A. Jolliffe[a,c,d], and Elizabeth J. New[a,c,d]

[a] Dr L. D. Adair, N. Trinh, Prof K. A. Jolliffe, A/Prof E. J. New
School of Chemistry
The University of Sydney
NSW 2006, Australia
E-mail: elizabeth.new@sydney.edu.au

[b] P. M. Vérité, Prof D. Jacquemin
CNRS
Université de Nantes
CEISAM UMR 6230
F-44000 Nantes, France

[c] Prof K. A. Jolliffe, A/Prof E. J. New
The University of Sydney Nano Institute (Sydney Nano)
The University of Sydney
NSW 2006, Australia

[d] Prof K. A. Jolliffe, A/Prof E. J. New
Australian Research Council Centre of Excellence for Innovations in Peptide and Protein Science
The University of Sydney
NSW 2006, Australia

Supporting information for this article is given via a link at the end of the document

Abstract: Fluorescent sensors are a vital research tool, enabling the study of intricate cellular processes in a sensitive manner. The design and synthesis of responsive and targeted probes is necessary to allow such processes to be interrogated in the cellular environment. This remains a challenge, and requires methods for functionalisation of fluorophores with multiple appendages for sensing and targeting groups. Methods to synthesise more structurally complex derivatives of fluorophores will expand their potential scope. Most known 4-amino-1,8-naphthalimides are only functionalised at imide and 4-positions, and structural modifications at additional positions will increase the breadth of their utility as responsive sensors. Here we evaluate methods for the incorporation of a hypoxia sensing group to 4-amino-1,8-naphthalimide. We developed an intermediate that allowed us to incorporate a sensing group, targeting group, and ICT donor to the naphthalimide core in a modular fashion. Synthetic strategies for attaching the hypoxia sensing group and how they affected the fluorescence of the naphthalimide were evaluated by photophysical characterisation and time-dependent density functional theory. We then rationally designed an extracellular hypoxia probe that could selectively image the hypoxic and necrotic region of tumour spheroids. Our results demonstrate the versatility of the naphthalimide scaffold and expand its utility. This approach to probe design will enable the flexible, efficient generation of selective, targeted fluorescent sensors for various biological purposes.

Introduction

Fluorescent sensing, particularly when applied to bioimaging, is a vital tool for studying chemical processes in biological systems. Many unanswered biochemical questions require selective, targeted, responsive fluorescent sensors and their development remains challenging.[1] Responsive fluorescent sensors typically comprise a sensing moiety tethered to a fluorophore, often through a conjugated linker. A particular challenge in the rapid development of new fluorescent sensors is the identification of fluorophore precursors to which sensing groups can be readily conjugated. To achieve this, it is important to identify fluorophore-linker scaffolds that enable facile conjugation of sensing groups, and for which the analyte induces a measurable fluorescence response.

4-Amino-1,8-naphthalimides are donor-acceptor molecules with an internal charge-transfer (ICT) excited state, and typically display strong fluorescence emission.[2] They are commonly used in bioimaging due to their chemical stability, photostability, high quantum yields, and large Stokes shifts.[3] Responsive 4-amino-1,8-naphthalimide based sensors have been reported for several analytes including metal ions,[4] anions,[5] and reactive small molecules.[6] Functionalisation at the imide or the 4-position predominates the literature (Figure 1), with additional functionalisation uncommon. Because of the limited scope for derivatisation to date, naphthalimides remain an underexplored class of fluorophore, and in order to maximise the potential of naphthalimides as responsive fluorescent sensors, it is essential to develop methods for functionalisation at other positions. Importantly, we identified the need to determine robust synthetic methods for introducing a broad range of sensor groups. This will allow rapid access to more structurally complex derivatives and enable more efficient development of a set of fluorescent sensors. We were particularly interested in a third point of attachment which could be functionalised orthogonally to the imide and 4-position.

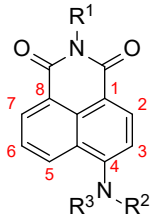

Figure 1. 4-Amino-1,8-naphthalimide structure.

We have previously reported several substituted 4-amino-1,8-naphthalimide derivatives with various simple structural modifications and found that the addition of substituents, particularly at the 6-position, expanded the range of emission wavelengths available.[7] An additional electron donating group at this position was shown to have a large impact as a secondary charge transfer (CT) donor, making it a promising position for incorporation of sensing groups. Among the compounds previously synthesised was a 6-bromo analogue, which had the potential to be used as a synthetic handle. This work aims to assess the synthetic strategies that are most promising for attaching sensing groups at this position, both in terms of optimal photophysical properties, and synthetic considerations.

We envisaged that the incorporation of nitro-aryl substituents onto the 4-amino-1,8-naphthalimide scaffold would provide a suitable model system in which to examine the above properties, anticipating that the resulting molecules would be useful probes for sensing hypoxic environments, since aromatic nitro compounds are known to be reduced to the corresponding aniline in hypoxic conditions.[8] Nitro groups generally quench fluorescence,[9] whereas in amine-containing fluorophores, strong fluorescence is common. This difference in fluorescence properties, coupled with the ease of reduction of the nitro group makes this an attractive strategy for the design of fluorogenic hypoxia probes and an ideal model system for our studies.[10]

Hypoxia develops in advanced solid tumours due to uncontrolled proliferation of cancer cells, resulting in regions that are distant from blood vessels, or possess inadequate tumoral vasculature, and therefore are starved of oxygen.[11] The development of these hypoxic regions can aid in tumorigenicity and promote changes that lead to disease progression, with acute hypoxia being associated with more aggressive tumour phenotypes and resistance to treatment.[12] Fluorescence imaging is a useful technique for imaging hypoxic regions of tumours as it is non-invasive, highly sensitive, and can provide spatiotemporal resolution. Other commonly-used methods for measuring hypoxia, such as microelectrodes, are invasive techniques.[13] To investigate the ease with which the nitro-aryl hypoxia sensing groups could be introduced onto the 4-amino-1,8-naphthalimide scaffold, together with the impact of different linkers on the photophysical properties of these systems we prepared a small series of 6-substituted-4-amino-1,8-naphthalimides and report here our investigations of these as fluorescent sensors of hypoxic microenvironments..

Results and Discussion

Design/Synthesis

We chose to incorporate the aryl-nitro functionality *via* four robust methodologies that are commonly used in synthetic chemistry, with readily available substrates: directly conjugated by a Suzuki-coupling, with an alkyne linker using a Sonogashira coupling, a triazole linker using Cu-catalysed azide-alkyne cycloaddition (CuAAC) click reaction, and by Buchwald-Hartwig amination. We designed four nitro-compounds (**1NO₂ - 4NO₂**), and their reduced aniline analogues (**1NH₂ - 4NH₂**) (Figure 2), to investigate how the aryl-nitro functionality is incorporated impacts the emission.

The reported synthesis of 6-bromonaphthalimide **7** contains a non-selective nitration and is low yielding for the desired regioisomer.[7] We therefore developed an alternative route to **7** with selective bromination of 4-nitro-1,8-naphthalic anhydride as the initial step. Commercially available 4-nitronaphthalic anhydride **5** was brominated regioselectively at the 6-position using NBS in strongly acidic conditions, giving the desired product **6** with no need for chromatographic purification. This substituted anhydride **6** is a key intermediate and allows for facile and

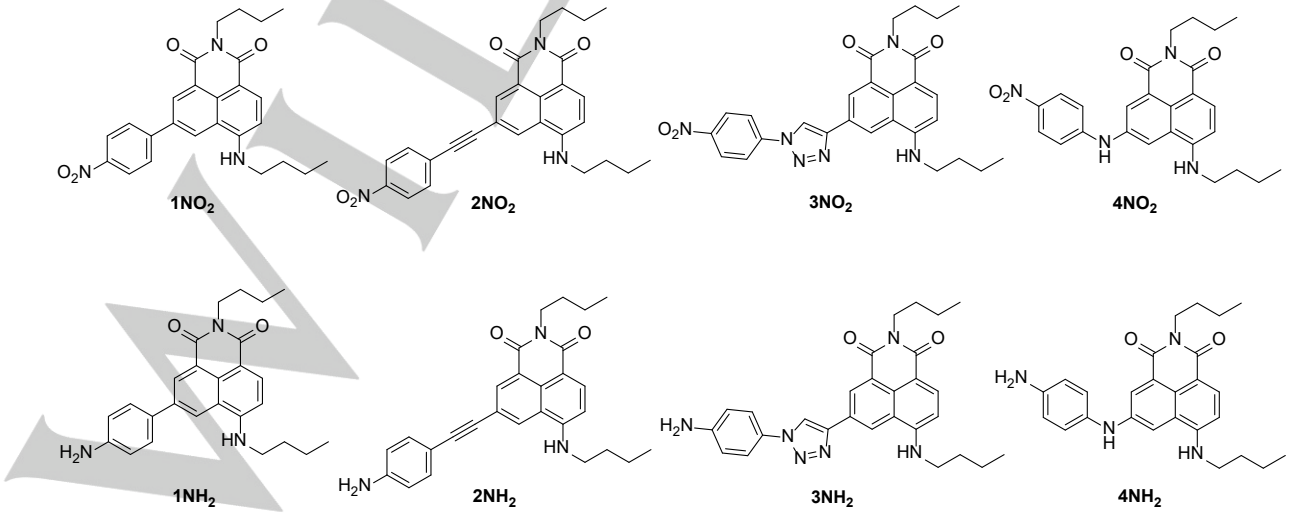

Figure 2. Structure of 6-aryl-nitro naphthalimides **1** – **4NO₂** and their reduced aniline derivatives **1** – **4NH₂**.

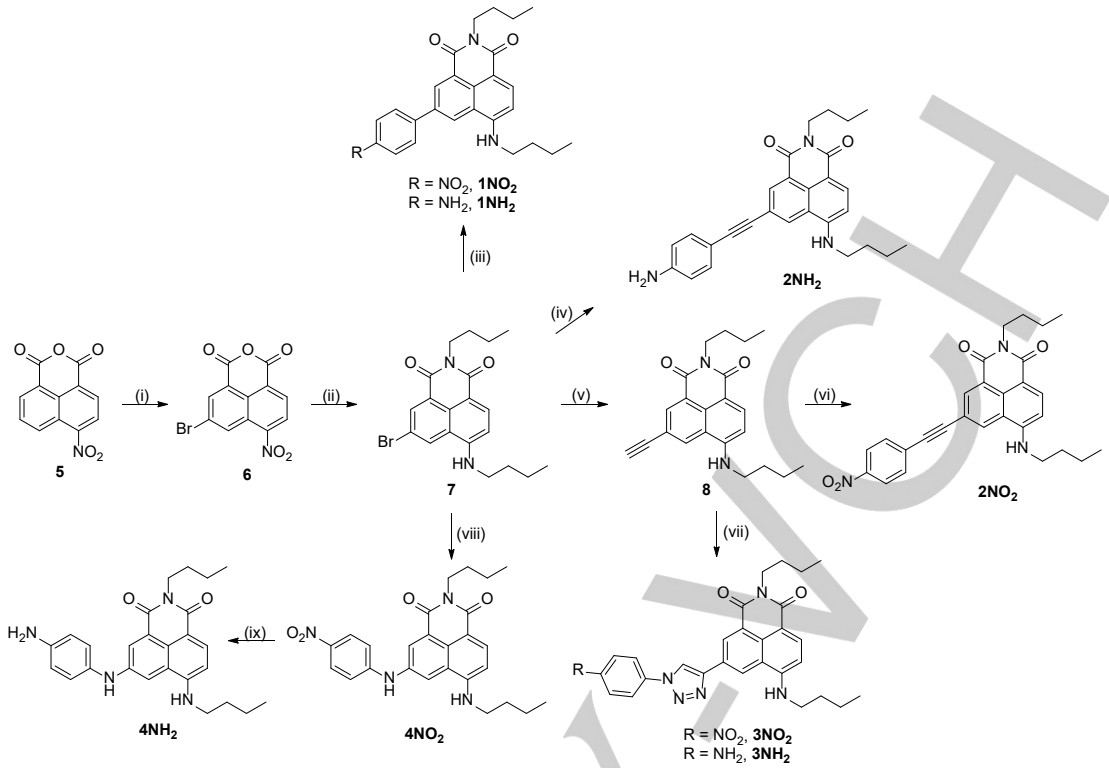

Scheme 1. Synthesis of **$1NO_2$** – **$4NO_2$** and **$1NH_2$ – $4NH_2$**. Reagents and conditions: (i) NBS, H_2SO_4, 60 °C, 93%; (ii) $^nBuNH_2$, EtOH, 80 °C, 55%; (iii) 4-nitrophenyl boronic acid or 4-aminophenyl boronic acid, $Pd(PPh_3)_4$, K_2CO_3, THF:H_2O, 70 °C, 41% (**$1NO_2$**), 98% (**$1NH_2$**); (iv) 4-ethynylaniline, $Pd(PPh_3)_2Cl_2$, CuI, THF:Et_3N, 80 °C, 76%; (v) 1. TMS-acetylene, $Pd(PPh_3)_2Cl_2$, CuI, THF:Et_3N, 80 °C, 2. TBAF, THF, 69% (over 2 steps); (vi) 4-bromo-1-nitrobenzene, $Pd(PPh_3)_2Cl_2$, CuI, THF:Et_3N, 80 °C, 62%; (vii) 1-azido-4-nitrobenzene or 4-azidoaniline, $CuSO_4.5H_2O$, NaAsc, Na_2CO_3, THF:H_2O, 66% (***$3NO_2$***), 98% (**$3NH_2$**); (viii) $Pd(OAc)_2$, RuPhos, Cs_2CO_3, toluene, 110 °C, 72%; (ix) Pd/C, NH_4CO_2H, EtOAc:MeOH, 98%.

selective functionalisation at each of the 4-, 6- and anhydride positions of the scaffold. Treatment with excess *n*-butylamine in EtOH gave bromo-naphthalimide **7**, in good overall yield leaving the 6-bromide handle for further functionalisation. Suzuki coupling of **7** with 4-nitrophenylboronic gave the desired product **$1NO_2$**. The aniline derivative **$1NH_2$** was similarly synthesised by Suzuki coupling, using 4-aminophenylboronic acid. Sonogashira coupling of **7** directly with 4-nitrophenylacetylene proved to be very low yielding. However, using TMS-acetylene as the coupling partner, followed by desilylation with TBAF, gave alkyne **8** in good yield over two steps. Subsequent coupling with 4-bromo-1-nitrobenzene gave the desired compound **$2NO_2$**. In contrast, 4-ethynylaniline was successfully coupled directly to the 6-bromonaphthalimide to generate the corresponding aniline analogue **$2NH_2$** in good yield. Acetylene **8** pleasingly also gave an intermediate to allow incorporation of the nitro-aryl functionality using CuAAC. 1-Azido-4-nitrobenzene and 4-azidoaniline were each prepared from the corresponding boronic acids *via* copper mediated conditions.[14] CuAAC reaction of acetylene **8** with 1-azido-4-nitrobenzene and 4-azidoaniline, respectively using $CuSO_4$ in THF:H_2O gave the desired triazoles **$3NO_2$** and **$3NH_2$** in excellent yield for both products. Buchwald-Hartwig amination of **7** using 4-nitroaniline gave the desired product **$4NO_2$**. Subsequent reduction of the nitro group using Pd-catalysed transfer hydrogenation with ammonium formate as the hydrogen source, gave the aniline derivative **$4NH_2$** (Scheme 1).

Photophysical studies

The photophysical properties of **$1NO_2$ - $4NO_2$** and **$1NH_2$ - $4NH_2$** were next measured in CH_2Cl_2 to determine both how these changed upon reduction of the nitro group and how these varied with the nature of the linker (Figure 3, Table 1). For the **NO_2** series, compounds **$3NO_2$**, and to a lesser extent compound **$1NO_2$**, show appreciable fluorescence, whereas **$2NO_2$** and **$4NO_2$** are almost completely quenched. In all four cases, reduction to the aniline resulted in a turn-on in fluorescence intensity rather than a change in emission wavelength. **$4NH_2$** has the weakest emission of the **NH_2** series, but also shows a significant bathochromic shift (Δ 30 nm).

Table 1. Comparison of excitation and emission maxima (in CH_2Cl_2) of **1** – **4** and unsubstituted N-butyl-4-butylamino-1,8-naphthalimide.

	λ_{ex} (nm)		λ_{em} (nm)	
Unsubstituted	421		503	
	NO_2	**NH_2**	**NO_2**	**NH_2**
1	442	440	507	509
2	445	450	520	509
3	444	446	511	512
4	456	459	497	527

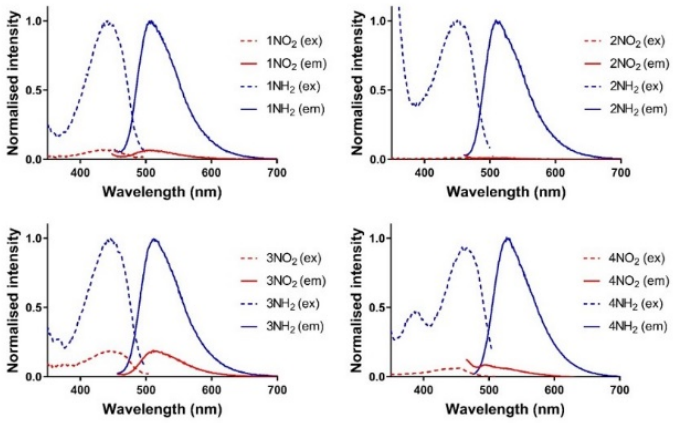

Figure 1: Excitation and emission spectra of **1** (1 μM in CH_2Cl_2, λ_{ex} 440 nm, λ_{em} 510 nm), **2** (1 μM in CH_2Cl_2, λ_{ex} 440 nm, λ_{em} 510 nm), **3** (1 μM in CH_2Cl_2, λ_{ex} 440 nm, λ_{em} 510 nm), **4** (5 μM in CH_2Cl_2, λ_{ex} 450 nm, λ_{em} 520 nm).

Computational studies

To shed more light on the photophysical properties of the compounds, we have used first principle calculations using a technique detailed in the SI and successfully applied to many dyes before.[15] Table 2 reports the computed positions of the lowest dipole-allowed transitions. The agreement between the theoretical and experimentally observed values is satisfactory: i) the mean absolute error is 0.20 eV, typical of such an approach;[15a] ii) theory overshoots the experimental value, which is the expected error sign when neglecting vibronic couplings;[15b] iii) the experimental fact that only **4NH₂** undergoes a significant bathochromic shift is reasonably reproduced.

Table 2. Comparison between theoretical (CC2, see the SI) and experimental excitation wavelengths given in eV.

	1NO₂	**2NO₂**	**3NO₂**	**4NO₂**	**1NH₂**	**2NH₂**	**3NH₂**	**4NH₂**
Theoretical	2.94	2.89	2.93	2.93	2.99	2.95	2.94	2.69
Experimental	2.70	2.72	2.71	2.78	2.75	2.72	2.71	2.58

Figure 4 represents the density difference plots for all compounds. In all cases, except for **4NH₂**, there is a significant ICT from the *N*-butylamino group (mostly in blue, donor) at position 4 to the core of the compound (mostly in red, acceptor). The side groups added at the 6-position play a minor role. **4NH₂** is a notable exception, with a strong ICT from the amine at the 6-position to the core of the molecule, an effect well in line with the large redshift measured for that compound. In **4NO₂**, there is likely a counterbalancing effect between the nitro and amino groups, and hence, a small overall effect is evident.

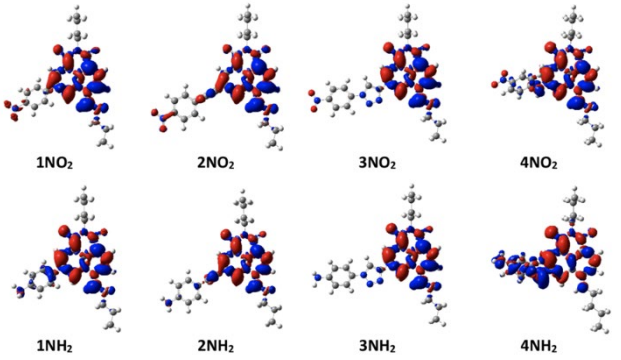

Figure 4: Density difference plots for the lowest transition in all compounds. The blue and red lobes represent regions of decrease and increase of density upon photon absorption. Contour threshold 8 × 10^{-4} au.

Next, we examined the emission behaviour. In the **NH₂** series, the S_1 optimisations led to small structural changes in **1NH₂** – **3NH₂** with computed emission wavelengths reasonably fitting the values that were observed experimentally. Again, **4NH₂** was an exception to this general rule, as the optimisation of the lowest state led to a very low-lying "theoretical fluorescence" at 1.64 eV with a large ICT effect involving the amine at the 6-position (as in the absorption figure 4). Such a low-lying transition will be dark experimentally, due to the well-known energy gap law, and hence the very low residual emission observed experimentally is likely coming from a side effect, e.g., an emission from S_2 or a fast emission from S_1 before its full relaxation. In that sense, the CT in **4NH₂** is too large and it consequently becomes an ineffective emitter. On the other hand, the three other **NH₂** compounds show the more classical behaviour of effective emitters with a more moderate CT, which fits with the experimental observations. As stated in the introduction, it is well known that nitro groups quench fluorescence, hence it is not surprising to see that all the **NO₂** compounds are less bright than their corresponding **NH₂** systems. Nevertheless, there are notable differences in the nitro series. For **1NO₂** – **4NO₂** the theoretical calculations predict fluorescence in the 2.52 – 2.62 eV range, which again fits the measurements (2.38 – 2.46 eV), with similar excited state topologies for all four compounds. Therefore, the experimental differences, and specifically the fact that (relative) quenching is much stronger in **1NO₂** and **2NO₂** than in **3NO₂**, should be explained by another phenomena. We reasoned that intersystem crossing (ISC) might be taking place and we have therefore computed S-T gaps on the lowest S_1 geometry for **1NO₂** – **4NO₂**. In all cases, the gap between S_1 and T_1 is very large (>0.6 eV) and therefore ISC is unlikely with the lowest triplet. In contrast, the S_1-T_2 gaps are very low in **4NO₂** (0.00 eV) and **2NO₂** (0.07 eV) and strong quenching would be expected, as is indeed found experimentally. In **3NO₂**, T_2 lies 0.49 eV higher than S_1 making ISC very unlikely, consistent with the relatively bright fluorescence observed. **1NO₂** is intermediate with a S_1-T_2 gap of 0.18 eV. These trends are clearly consistent with the experimental measurements.

With these results we then evaluated which scaffold would be optimal for a useful hypoxia sensor. As compound **3** had significant fluorescence in the **3NO₂** form (Φ 0.06 in EtOH, Table S1), reducing the turn on response and compound **4NH₂** was not bright enough to be a promising candidate, these scaffolds were ruled out. The turn-on response for compounds **1** and **2** made them the most promising candidates for a hypoxia probe. Non-radiative decay in 4-amino-1,8-naphthalimides is generally increased in aqueous solvents,[16] but interestingly, the fluorescence of **2NH₂** was significantly quenched in aqueous buffer, whereas **1NH₂** remained bright (Figure 5). **1NH₂** was also the scaffold with the highest quantum yield (Φ 0.42 in EtOH, Table S1).

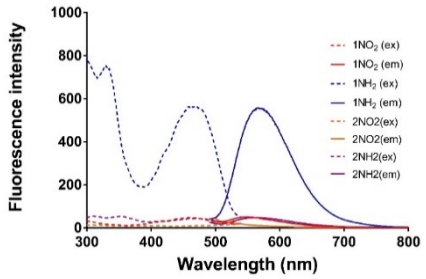

Figure 5. Excitation and Emission spectra of **1** and **2** (50 μM in HEPES buffer 100 mM pH 7.4)

Preliminary biological studies

1NO₂ was therefore the most promising hypoxia sensor amongst those synthesised, and its potential utility was therefore evaluated in preliminary biological studies. Firstly, the cytoxicity of **1NO₂** was assessed by Alamar blue assay, which confirmed that the compound was not toxic to DLD-1 cells (Figure S3). Next, we carried out a preliminary imaging experiment with a tumour spheroid model. DLD-1 cells were allowed to grow into three-dimensional spheroids of varying size. Such systems develop a hypoxic region which is far from the oxygenated cell culture media, mimicking the environment of a solid tumour. Imaging of spheroids incubated with **1NO₂** showed high fluorescence intensity at the periphery of the spheroid, consistent with rapid uptake of probe into the outer cells, preventing diffusion into the hypoxic region of the spheroid (Figure S4). Furthermore, the bright fluorescence intensity observed indicates that **1NO₂** is too easily reduced in the highly reducing intracellular environment, consistent with a previous work.[8] We therefore sought to modify this system to enable imaging of the hypoxic region by developing an extracellular version of **1NO₂**, in which cellular uptake is inhibited through the incorporation of an aspartic acid group that would exist in the dicarboxylate form at biologically relevant pH.

Synthesis of extracellular analogue

We envisaged that naphthalic anhydride **6** could be functionalised selectively at the anhydride, 4-, and 6- position. This would allow for modular, orthogonal incorporation of a targeting group, sensing group, and ICT donor. We first formed naphthalimide **9** through selective condensation of anhydride **6** with aspartic acid dimethyl ester. The use of 1,4-dioxane as solvent allowed for selective reaction of the amine at the imide position, giving **9** as the sole product in good yield, with no chromatographic purification. Substitution of the nitro group upon treatment with *n*-butylamine in MeCN gave the bromide **10** in excellent yield. The bromide was then subjected to Suzuki coupling with 4-nitrophenylboronic acid to give di-ester **11**, followed by basic hydrolysis of the methyl esters to give the final extracellular hypoxia probe **Asp-1NO₂** (Scheme 2).

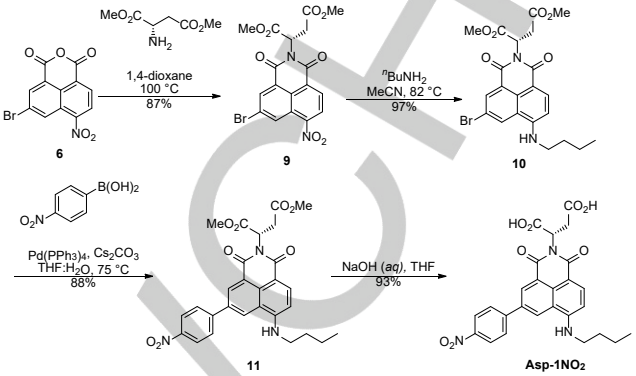

Scheme 2. Synthesis of extracellular hypoxia sensor **Asp-1NO₂**.

With probe **Asp-1NO₂** in hand, we first investigated the fluorescence response by chemical reduction with sodium dithionite in aqueous solution. **Asp-1NO₂** showed a strong fluorescence emission increase at 550 nm upon reduction (Figure 6). The cytotoxicity to DLD-1 cells was assessed, by Alamar blue assay, and **Asp-1NO₂** was shown to be non-toxic to cells after 24 h incubation, indicating its suitability for biological studies (Figure S3).

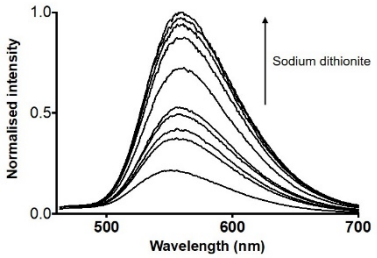

Figure 6. Fluorescence titration of Asp-1NO₂ with increasing concentration of sodium dithionite (10 μM in PBS pH 7.4, λ_{ex} 445 nm).

Asp-1NO₂ was then used in an analogous imaging experiment to that performed with **1NO₂**. Spheroids of varying size were incubated with probe **Asp-1NO₂** then imaged and a turn-on in fluorescence was observed approximately 100 μm from the spheroid surface. This distance corresponds to the limit of where oxygen can diffuse, and the beginning of the hypoxic region.[17] In the larger spheroids, fluorescence was also observed at the very centre of the spheroid, this corresponds to the necrotic region. In the smallest spheroid, which is lacking a hypoxic region, no fluorescence was observed demonstrating the selectivity for hypoxic microenvironments (Figure 7). The clear differences in fluorescence of **1NO₂** and **Asp-1NO₂** within spheroids (Figures S4, 7) confirm the role of the aspartic acid group in enabling the probe to travel between cells into the centre of the spheroid.

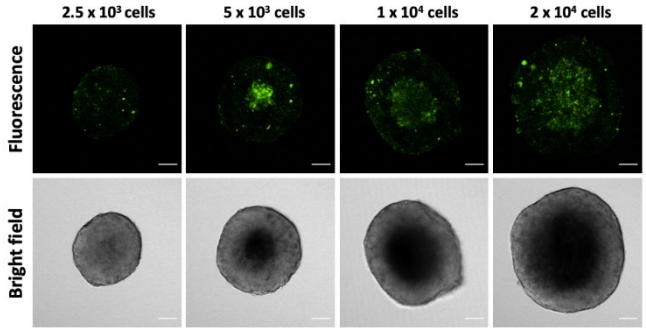

Figure 7. Confocal microscopy images of DLD-1 spheroids of varying sizes treated with 50 μM of probe **Asp-1NO$_2$** (scale bar represents 100 μm).

Conclusion

We have demonstrated a versatile approach to the synthesis of 4-amino-1,8-napthhalimide based probes and a flexible approach to incorporation of sensing groups to the naphthalimide core using simple, modular chemistry. All linkers gave rise to a change in fluorescence intensity, and from these results we expect various sensing groups could be incorporated using an aryl-linker at the 6-position and make effective, responsive sensors. Theoretical calculations allowed us to rationalise the weak fluorescence of 4NH$_2$ as due to a too strong excited-state relaxation and also evidenced differences in the singlet-triplet gaps that nicely correlate with experimental fluorescence quenching for the nitro series.

For use in sensing hypoxia, the Suzuki coupled product **1NO$_2$** was determined to be the optimal structure, as this had the highest quantum yield, a large turn-on response upon reduction to **1NH$_2$**, and was the most intensely fluorescent in aqueous media. Using a modular approach, we have selectively functionalised the naphthalimide core with a targeting group at the imide position, amino donor at the 4-position, and a sensing group at the 6-position to synthesise the rationally designed extracellular hypoxia naphthalimide based probe **Asp-1NO$_2$**. **Asp-1NO$_2$** was used to successfully image the hypoxic and necrotic regions of tumour cell spheroids. One challenge for the use of green emitting fluorophores for tumour imaging, however, is their limited tissue penetration. Two-photon microscopy has been employed to address this issue for several naphthalimide based sensors, and could allow for **Asp-1NO$_2$** to be used for imaging in tissues.[6c, 18] Our ongoing research also involves the development of more red-shifted probes.

This work further illustrates the versatility of the naphthalimide scaffold: we could readily substitute the group at the imide position to target any cell type or sub-cellular organelle, and easily append a variety of sensing groups. This approach to naphthalimide based probe design and synthesis is flexible allowing for the efficient generation of targeted, selective fluorescent probes and work is underway in applying this approach to the synthesis of various probes for biological purposes.

Experimental Section

Full experimental details are included in the ESI

Acknowledgements

The authors would like to acknowledge the Australian Research Council (DP180101353) for funding, the Westpac Scholars Trust for a Research Fellowship (EJN), the University of Sydney for a SOAR Fellowship (EJN) and the Australian Government for a Research Training Program Scholarship (NT). We acknowledge the scientific and technical assistance of Sydney Analytical, and the Australian Microscopy and Microanalysis Research Facility at the Australian Centre for Microscopy and Microanalysis (ACMM).

Keywords: fluorescent sensor • hypoxia • 4-amino-1,8-naphthalimide

[1] E. J. New, *ACS Sensors* **2016**, *1*, 328-333.
[2] a) S. Saha, A. Samanta, *The Journal of Physical Chemistry A* **2002**, *106*, 4763-4771; b) P. Kucheryavy, G. Li, S. Vyas, C. Hadad, K. D. Glusac, *The Journal of Physical Chemistry A* **2009**, *113*, 6453-6461.
[3] R. M. Duke, E. B. Veale, F. M. Pfeffer, P. E. Kruger, T. Gunnlaugsson, *Chemical Society Reviews* **2010**, *39*, 3936-3953.
[4] a) K. Hanaoka, Y. Muramatsu, Y. Urano, T. Terai, T. Nagano, *Chemistry – A European Journal* **2010**, *16*, 568-572; b) Z. Xu, K.-H. Baek, H. N. Kim, J. Cui, X. Qian, D. R. Spring, I. Shin, J. Yoon, *Journal of the American Chemical Society* **2010**, *132*, 601-610; c) R. K. Jackson, Y. Shi, X. Yao, S. C. Burdette, *Dalton Transactions* **2010**, *39*, 4155-4161; d) Z. Xu, J. Yoon, D. R. Spring, *Chemical Communications* **2010**, *46*, 2563-2565; e) Z. Xu, Y. Xiao, X. Qian, J. Cui, D. Cui, *Organic Letters* **2005**, *7*, 889-892; f) R. Parkesh, T. Clive Lee, T. Gunnlaugsson, *Org Biomol Chem* **2007**, *5*, 310-317.
[5] a) Z. Xu, Y.-Y. Ren, X. Fan, S. Cheng, Q. Xu, L. Xu, *Tetrahedron* **2015**, *71*, 5055-5058; b) S. N. Berry, V. Soto-Cerrato, E. N. W. Howe, H. J. Clarke, I. Mistry, A. Tavassoli, Y.-T. Chang, R. Pérez-Tomás, P. A. Gale, *Chemical Science* **2016**, *7*, 5069-5077; c) X. Sun, S. D. Dahlhauser, E. V. Anslyn, *Journal of the American Chemical Society* **2017**, *139*, 4635-4638; d) F. M. Pfeffer, A. M. Buschgens, N. W. Barnett, T. Gunnlaugsson, P. E. Kruger, *Tetrahedron Letters* **2005**, *46*, 6579-6584; e) J. F. Zhang, C. S. Lim, S. Bhuniya, B. R. Cho, J. S. Kim, *Organic Letters* **2011**, *13*, 1190-1193.
[6] a) D. Srikun, E. W. Miller, D. W. Domaille, C. J. Chang, *Journal of the American Chemical Society* **2008**, *130*, 4596-4597; b) X. Sun, Q. Xu, G. Kim, S. E. Flower, J. P. Lowe, J. Yoon, J. S. Fossey, X. Qian, S. D. Bull, T. D. James, *Chemical Science* **2014**, *5*, 3368-3373; c) J. Fan, Z. Han, Y. Kang, X. Peng, *Scientific Reports* **2016**, *6*, 19562; d) L. Zhang, W.-q. Meng, L. Lu, Y.-S. Xue, C. Li, F. Zou, Y. Liu, J. Zhao, *Scientific Reports* **2014**, *4*, 5870; e) X.-L. Liu, X.-J. Du, C.-G. Dai, Q.-H. Song, *The Journal of Organic Chemistry* **2014**, *79*, 9481-9489.
[7] K. G. Leslie, D. Jacquemin, E. J. New, K. A. Jolliffe, *Chem-Eur J* **2018**, *24*, 5569-5573.
[8] K. Yang, K. G. Leslie, S. Y. Kim, B. Kalionis, W. Chrzanowski, K. A. Jolliffe, E. J. New, *Org Biomol Chem* **2018**, *16*, 619-624.

[9] E. Collado-Fregoso, J. S. Zugazagoitia, E. F. Plaza-Medina, J. Peon, *J Phys Chem A* **2009**, *113*, 13498-13508.
[10] R. B. P. Elmes, *Chemical Communications* **2016**, *52*, 8935-8956.
[11] K. L. Eales, K. E. R. Hollinshead, D. A. Tennant, *Oncogenesis* **2016**, *5*, e190-e190.
[12] aJ. Pouysségur, F. Dayan, N. M. Mazure, *Nature* **2006**, *441*, 437-443; bM. Höckel, P. Vaupel, *JNCI: Journal of the National Cancer Institute* **2001**, *93*, 266-276.
[13] X. Sun, G. Niu, N. Chan, B. Shen, X. Chen, *Molecular Imaging and Biology* **2011**, *13*, 399-410.
[14] K. D. Grimes, A. Gupte, C. C. Aldrich, *Synthesis-Stuttgart* **2010**, 1441-1448.
[15] a) D. Jacquemin, I. Duchemin, X. Blase, *Journal of Chemical Theory and Computation* **2015**, *11*, 5340-5359; b) A. D. Laurent, C. Adamo, D. Jacquemin, *Physical Chemistry Chemical Physics* **2014**, *16*, 14334-14356.
[16] D. Yuan, R. G. Brown, *The Journal of Physical Chemistry A* **1997**, *101*, 3461-3466.
[17] A. J. Franko, R. M. Sutherland, *Radiation Research* **1979**, *79*, 439-453.
[18] a) B. Zhu, P. Li, W. Shu, X. Wang, C. Liu, Y. Wang, Z. Wang, Y. Wang, B. Tang, *Analytical Chemistry* **2016**, *88*, 12532-12538; b) Z.-R. Dai, G.-B. Ge, L. Feng, J. Ning, L.-H. Hu, Q. Jin, D.-D. Wang, X. Lv, T.-Y. Dou, J.-N. Cui, L. Yang, *Journal of the American Chemical Society* **2015**, *137*, 14488-14495.

Entry for the Table of Contents

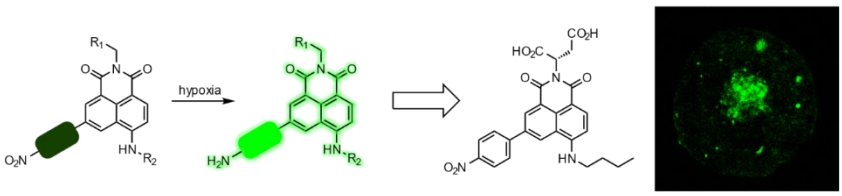

Synthetically-versatile fluorophore cores will enable the rapid preparation of novel responsive fluorescent sensors. We have developed methods for incorporating sensing groups at the 6-position of 4-amino-1,8-naphthalimide, and have used this to prepare a set of hypoxia-responsive fluorophores. We further demonstrate the versatility of this scaffold by preparing an extracellular analogue that can image the hypoxic region of a tumour spheroid.

Institute and/or researcher Twitter usernames: @liamthechemist @kate_jolliffe @lizjnew @newgroupchem @sydneychemistry

Electronic Supplementary Information

for

Synthesis of nitro-aryl functionalised 4-amino-1,8-naphthalimides and their evaluation as fluorescent hypoxia sensors

Liam Adair[1], Natalie Trinh[1], Pauline M. Vérité[2], Denis Jacquemin[2], Katrina A. Jolliffe[1,3,4] and Elizabeth J. New[1,3,4]

1. The University of Sydney, School of Chemistry, NSW 2006, Australia
2. Université de Nantes, CNRS, CEISAM UMR 6230, F-44000 Nantes, France
3. The University of Sydney Nano Institute (Sydney Nano), The University of Sydney, NSW 2006, Australia
4. Australian Research Council Centre of Excellence for Innovations in Peptide and Protein Science, University of Sydney, NSW 2006, Australia

Table of Contents

Synthetic methods

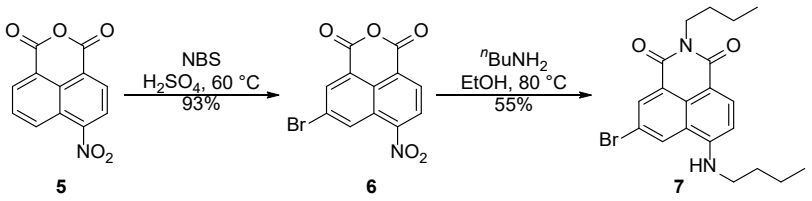

Scheme S1: Synthesis of **7**.

3-Bromo-5-nitro-1,8-naphthalic anhydride

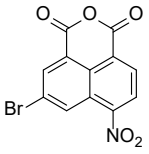

4-Nitronaphthalic anhydride (2.00 g, 8.20 mmol) was dissolved in conc. H_2SO_4 (40 mL). NBS (1.60 g, 9.00 mmol) was added and the resultant mixture heated to 60 °C and stirred for 16 h. The reaction mixture was then cooled and poured over ice, then extracted with CH_2Cl_2 (3 × 200 mL). The combined organics were dried (Na_2SO_4), filtered, and concentrated *in vacuo* to give the desired product as a pale yellow solid (2.45 g, 93%).

^{1}H NMR (500 MHz, $CDCl_3$): δ 9.17 (1H, d, *J* = 1.8 Hz), 8.84 (1H, d, *J* = 1.8 Hz), 8.75 (1H, d, *J* = 8.0 Hz), 8.54 (1H, d, *J* = 8.0 Hz).

^{13}C NMR (125 MHz, $CDCl_3$): δ 158.1, 158.0, 148.9, 137.6, 133.0, 132.1, 129.6, 125.6, 125.5, 125.0, 123.5, 120.6.

HRMS (APPI): calculated for $C_{12}H_4N_1O_5Br$ $[M]^+$ m/z 320.9267, observed 320.9267.

N-Butyl-3-bromo-5-butylamino-1,8-naphthalimide

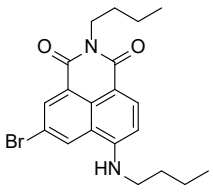

3-Bromo-5-nitro-1,8-naphthalic anhydride (500 mg, 1.55 mmol) was dissolved in EtOH (30 mL) under a nitrogen atmosphere. ^{n}BuNH$_2$ (0.31 mL, 3.10 mmol) was added, and the resultant mixture heated to reflux, and stirred for 16 h. The reaction mixture was cooled, diluted with 0.2 M HCl (*aq*) (200 mL), and extracted with CH_2Cl_2 (3 x 200 mL). The combined organic extracts were dried (Na_2SO_4), filtered, and concentrated *in vacuo*. Purification *via* automated flash chromatography (silica gel, 0 - 8% EtOAc in hexanes) gave the desired product as a bright orange solid (346 mg, 55%).

^{1}H NMR (500 MHz, $CDCl_3$): δ 8.57 (1H, d, *J* = 1.8 Hz), 8.41 (1H, d, *J* = 8.4 Hz), 8.19 (1H, d, *J* = 1.5 Hz), 6.72 (1H, d, *J* = 8.4 Hz), 4.15 - 4.12 (2H, m), 3.41 - 3.38 (2H, m), 1.84 - 1.78 (2H, m), 1.72 - 1.66 (2H, m), 1.58 - 1.50 (2H, m), 1.46 - 1.39 (2H, m), 1.03 (3H, t, *J* = 7.4 Hz), 0.96 (3H, t, *J* = 7.4 Hz).

^{13}C NMR (125 MHz, $CDCl_3$): δ 163.6, 163.5, 148.4, 134.5, 133.7, 128.2, 128.2, 124.8, 121.7, 118.6, 110.4, 105.2, 43.6, 40.1, 30.3, 20.5, 20.4, 20.4, 13.9, 13.8.

The data observed is in accordance with literature values.[1]

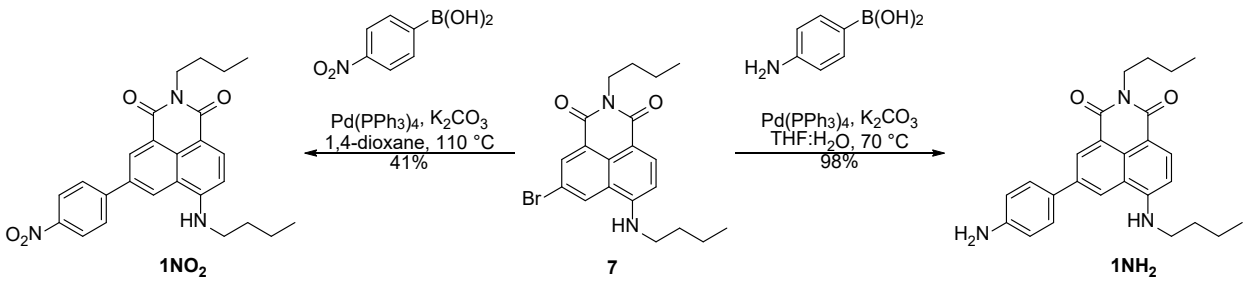

Scheme S2: Synthesis of **$1NO_2$** and **$1NH_2$**.

***N*-Butyl-4-butylamino-6-(4-nitrophenyl)-1,8-naphthalimide**

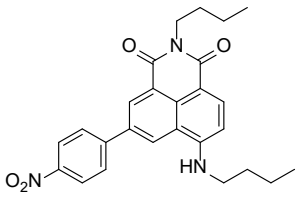

$1NO_2$

N-Butyl-4-butylamino-3-bromo-1,8-naphthalimide (100 mg, 0.24 mmol) and 4-nitrophenyl boronic acid (50 mg, 0.30 mmol) were dissolved in degassed 1,4-dioxane (8 mL), under a nitrogen atmosphere. To the resultant solution $Pd(PPh_3)_4$ (28 mg, 10 mol%) and K_2CO_3 (100 mg, 0.72 mmol) were added and the reaction mixture was heated to reflux and stirred for 36 h. The reaction was then diluted with EtOAc (50 mL), washed with H_2O (50 mL), brine (50 mL), then dried (Na_2SO_4), filtered, and concentrated *in vacuo*. Purification *via* automated flash chromatography (silica gel 0 - 8% EtOAc in hexanes) gave the desired product as a bright orange solid (44 mg, 41%).

^{1}H NMR (500 MHz, $CDCl_3$): δ 8.80 (1H, d, *J* = 1.6 Hz), 8.49 (1H, d, *J* = 8.4 Hz), 8.34 - 8.31 (2H, m), 8.26 (1H, s), 7.86 (2H, d, *J* = 8.7 Hz), 6.80 (1H, d, *J* = 7.2 Hz), 4.20 - 4.17 (2H, m), 3.49 - 3.46 (2H, m), 1.89 - 1.83 (2H, m), 1.75 - 1.69 (2H, m), 1.60 - 1.53 (2H, m), 1.49 - 1.41 (2H, m), 1.05 (3H, t, *J* = 7.4 Hz), 0.98 (3H, t, *J* = 7.4 Hz).

^{13}C NMR (125 MHz, $CDCl_3$): δ 164.4, 163.9, 149.8, 147.4, 146.3, 135.3, 135.0, 129.9, 129.5, 128.2, 124.4, 124.3, 124.1, 120.7, 110.2, 105.2, 43.7, 40.1, 31.0, 30.3, 20.4, 20.4, 13.9.

HRMS (ESI): calculated for $C_{26}H_{27}N_3O_4$ $[M+Na]^+$ m/z 468.1894, observed 468.1900.

***N*-Butyl-4-butylamino-6-(4-aminophenyl)-1,8-naphthalimide**

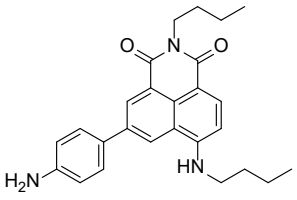

1NH$_2$

N-Butyl-3-bromo-5-butylamino-1,8-naphthalimide (50 mg, 0.12 mmol), 4-aminophenylboronic acid HCl (26 mg, 0.15 mmol), K_2CO_3 (50 mg, 0.36 mmol), and $Pd(PPh_3)_4$ (14 mg, 10 mol%) were dissolved in degassed THF:H_2O (10:3, 5 mL), under a nitrogen atmosphere. The resultant mixture was heated to reflux and stirred for 4 h. The reaction mixture was diluted with EtOAc (25 mL), washed with H_2O (25 mL), brine (25 mL), the organic dried ($MgSO_4$), filtered, and concentrated *in vacuo*. Purification *via* automated flash chromatography (silica gel, 5 - 20% EtOAc in hexanes) gave the desired product as an orange solid (49 mg, 98%).

^{1}H NMR (400 MHz, $CDCl_3$) δ: 8.75 (1H, s), 8.42 (1H, d, *J* = 8.4 Hz), 8.11 (1H, s), 7.53 (2H, d, *J* = 7.8 Hz), 6.84 (2H, d, *J* = 7.8 Hz), 6.72 (1H, d, *J* = 8.4 Hz), 5.37 (1H, br. s), 4.21 - 4.17 (2H, m), 3.45 - 3.42 (2H, m), 1.87 - 1.80 (2H, m), 1.77 - 1.70 (2H, m), 1.60 - 1.51 (2H, m), 1.51 - 1.42 (2H, m), 1.05 (3H, t, *J* = 7.4 Hz), 0.99 (3H, t, *J* = 7.4 Hz).

^{13}C NMR (100 MHz, $CDCl_3$): 164.8, 164.2, 149.4, 146.1, 137.9, 133.7, 130.4, 130.1, 128.3, 123.5, 122.4, 120.7, 115.8, 115.8, 110.3, 104.5, 43.5, 40.0, 31.1, 30.4, 20.4, 20.4, 13.9, 13.9.

HRMS (APPI): calculated for $C_{26}H_{29}N_3O_2$ $[M]^+$ m/z 415.2254, observed 415.2254.

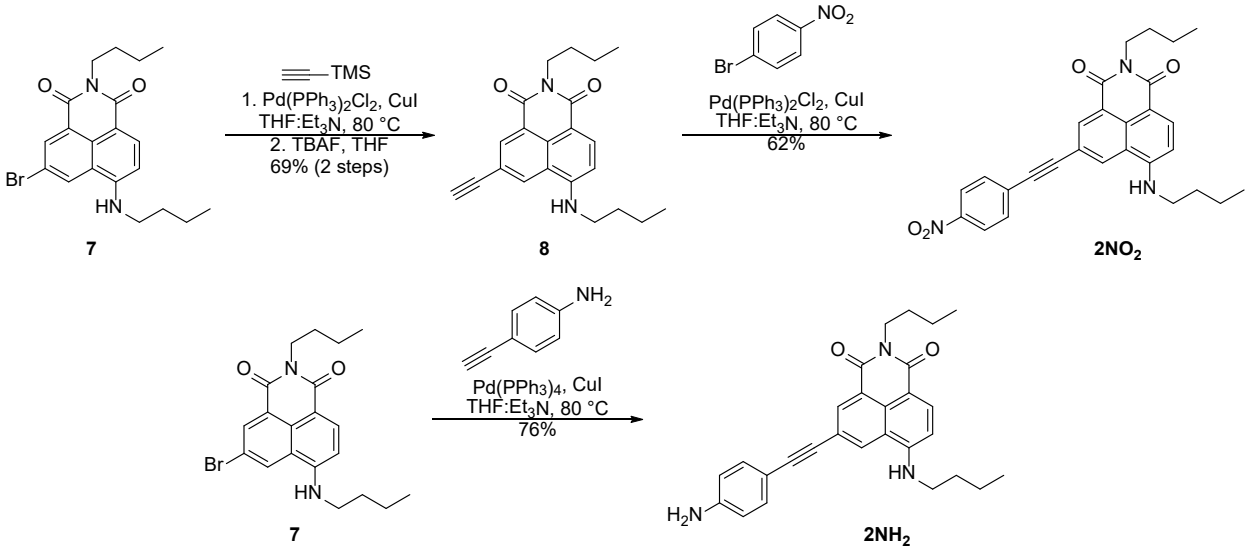

Scheme S3: Synthesis of **2NO$_2$** and **2NH$_2$**.

***N*-Butyl-4-butylamino-6-ethynyl-1,8-naphthalimide**

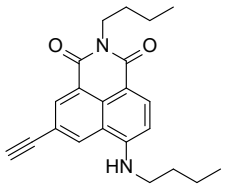

8

N-Butyl-4-butylamino-3-bromo-1,8-naphthalimide (403 mg, 1.00 mmol) and TMS-acetylene (625 µL, 5.00 mmol) were dissolved in degassed anhydrous THF:Et_3N (1:1, 30 mL), under a nitrogen atmosphere. $Pd(PPh_3)_2Cl_2$ (70 mg, 10 mol%) and CuI (38 mg, 20 mol%) were added, and the resultant mixture heated to reflux and stirred for 16 h. The reaction was then diluted with EtOAc (200 mL) then washed with H_2O (100 mL × 2), brine (100 mL), and the organic dried (Na_2SO_4), filtered, and concentrated *in vacuo.* Purification *via* automated flash chromatography (silica gel, 0 - 8% EtOAc in hexanes) gave the TMS-protected acetylene as a brown solid (354 mg, 84%). The purified intermediate was dissolved in anhydrous THF (15 mL), under a nitrogen atmosphere. TBAF (1M in THF, 1.26 mL, 1.26 mmol) was added dropwise, and the resultant mixture stirred for 16 h. Saturated NH_4Cl (*aq*) (40 mL) was added followed by EtOAc (50 mL). The aqueous layer was removed, and the organic washed with brine (50 mL), then dried (Na_2SO_4), filtered, and concentrated *in vacuo*. Purification *via* automated flash chromatography (silica gel, 0-12% EtOAc in hexanes) gave the desired product as an orange solid (foam) (241 mg, 82%) (69% over 2 steps).

^{1}H NMR ($CDCl_3$, 500 MHz): δ 8.60 (1H, d, *J* = 1.3 Hz), 8.44 (1H, d, *J* = 8.5 Hz), 8.18 (1H, d, *J* = 1.1 Hz), 6.72 (1H, d, *J* = 8.5 Hz), 5.26 (1H, br. s), 4.18 - 4.11 (2H, m), 3.41 (2H,m), 3.22 (1H, s), 1.84 - 1.78 (2H, m), 1.73 - 1.66 (2H, m), 1.58 - 1.51 (2H, m), 1.47 - 1.40 (2H, m), 1.04 (3H, t, *J* = 7.4 Hz), 0.97 (3H, t, *J* = 7.4 Hz).

^{13}C NMR (125 MHz, $CDCl_3$): δ 163.9, 163.8, 149.0, 135.1, 133.7, 129.3, 129.3, 123.5, 119.9, 118.5, 110.2, 104.9, 82.6, 78.6, 43.5, 40.1, 31.0, 30.3, 20.4, 20.3, 13.9, 13.8.

HRMS (ESI): calculated for $C_{22}H_{20}N_2O_2$ $[M+H]^+$ m/z 349.1911, observed 349.1908.

***N*-Butyl-4-butylamino-6-((4-nitrophenyl)ethynyl)-1,8-naphthalimide**

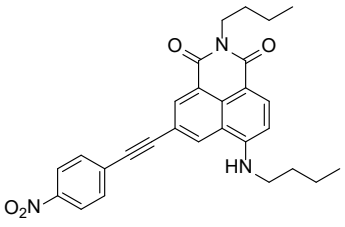

2NO$_2$

N-Butyl-4-butylamino-6-ethynyl-1,8-naphthalimide (40 mg, 0.12 mmol), 4-bromo-1-nitrobenzene (30 mg, 0.15 mmol), CuI (4.6 mg, 20 mol%), and $Pd(PPh_3)_4$ (14 mg, 10 mol%) were dissolved in degassed anhydrous THF:Et_3N (5:1, 3 mL), under a nitrogen atmosphere. The resultant mixture was heated to reflux and stirred for 16 h. The reaction mixture was then cooled to rt, diluted with EtOAc (20 mL), washed with H_2O (20 mL), brine (20 mL), dried (Na_2SO_4), filtered, and concentrated *in vacuo*. Purification *via* automated flash chromatography (silica gel, 2 - 10% EtOAc in hexanes) gave the desired product as a red solid (35 mg, 62%).

^{1}H NMR (500 MHz, $CDCl_3$): δ 8.66 (1H, s), 8.47 (1H, d, *J* = 8.4 Hz), 8.26 - 8.24 (3H, m), 7.69 (2H, d, *J* = 7.8 Hz), 6.76 (1H, d, *J* = 8.4 Hz), 4.17 (2H, t, *J* = 7.4 Hz), 3.44 (2H, t, *J* = 7.2 Hz), 1.87 - 1.81 (2H, m), 1.74 - 1.68 (2H, m), 1.61 - 1.53 (2H, m), 1.48 - 1.41 (2H, m), 1.05 (3H, t, *J* = 7.3 Hz), 0.98 (3H, t, *J* = 7.2 Hz).

^{13}C NMR (125 MHz, $CDCl_3$): δ 163.9, 163.8, 149.2, 147.3, 135.4, 133.4, 132.4, 129.5, 129.5, 129.0, 123.8, 123.7, 120.1, 118.5, 110.3, 105.2, 93.5, 88.8, 43.6, 40.1, 31.0, 30.3, 20.4, 20.4, 13.9, 13.9.

HRMS (APPI): calculated for $C_{28}H_{27}N_3O_4$ $[M]^+$ m/z 469.1996, observed 469.1996.

***N*-Butyl-4-butylamino-6-((4-aminophenyl)ethynyl)-1,8-naphthalimide**

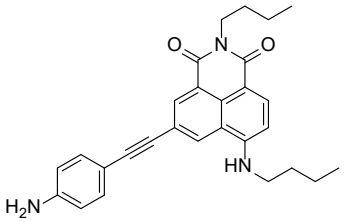

$2NH_2$

N-Butyl-3-bromo-5-butylamino-1,8-naphthalimide (50 mg, 0.12 mmol), 4-ethynylaniline (18 mg, 0.15 mmol), $Pd(PPh_3)_4$ (14 mg, 10 mol%), and CuI (4.6 mg, 20 mol%) were dissolved in degassed anhydrous THF:Et_3N (5:1, 4 mL), under a nitrogen atmosphere. The resultant mixture was heated to reflux and stirred for 36 h. The reaction mixture was then cooled to rt, diluted with EtOAc (20 mL), washed with H_2O (20 mL), brine (20 mL), dried ($MgSO_4$), filtered, and concentrated *in vacuo*. Purification *via* automated flash chromatography (silica gel, 5 - 30% EtOAc in hexanes) gave the desired product as a dark orange solid (40 mg, 76%).

^{1}H NMR (500 MHz, $CDCl_3$): δ 8.60 (1H, s), 8.40 (1H, d. *J* = 8.4 Hz), 8.14 (1H, s), 7.37 (2H, d, *J* = 7.8 Hz), 6.69 (1H, d, *J* = 8.4 Hz), 6.65 (2H, br. d, *J* = 6.0 Hz), 5.31 (1H, s), 4.17 - 4.14 (2H, m), 3.42 - 3.38 (2H, m), 1.83 - 1.78 (2H, m), 1.74 - 1.67 (2H, m), 1.58 - 1.51 (2H, m), 1.47 - 1.40 (2H, m), 1.03 (3H, t, *J* = 7.3 Hz), 0.96 (3H, t, *J* = 7.4 Hz).

^{13}C NMR (125 MHz, $CDCl_3$): δ 164.1, 164.0, 149.0, 134.5, 133.6, 133.1, 133.1, 128.6, 128.0, 123.3, 120.6, 120.1, 114.8, 111.8, 110.2, 104.7, 91.9, 86.6, 43.5, 40.0, 31.0, 30.3, 20.4, 20.4, 13.9, 13.8.

HRMS (APPI): calculated for $C_{28}H_{29}N_3O_2$ $[M]^+$ m/z 439.2254, observed 439.2254.

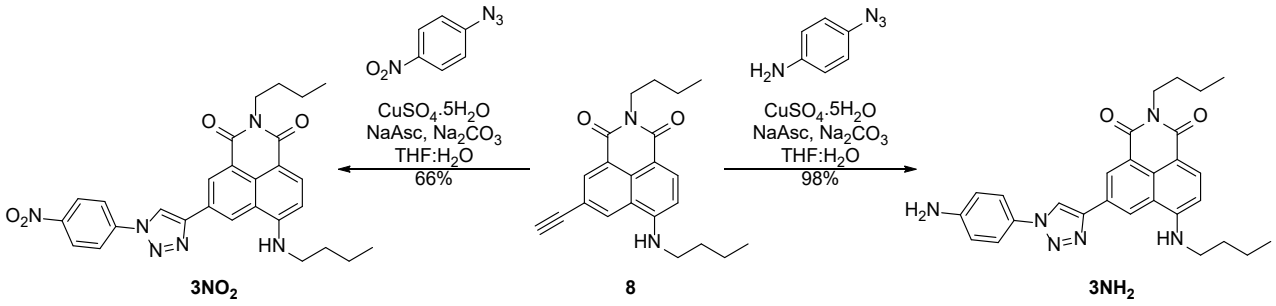

$3NO_2$ **8** **$3NH_2$**

Scheme S4: Synthesis of **$3NO_2$** and **$3NH_2$**.

1-Azido-4-nitrobenzene

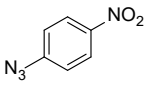

4-Nitrophenylboronic acid (83 mg, 0.50 mmol) was dissolved in MeOH (2.5 mL), under air. NaN_3 (49 mg, 0.75 mmol) and $Cu(OAc)_2$ (10 mg, 0.05 mmol) were added and the reaction mixture was heated to 55 °C and stirred for 16 h. The reaction mixture was then diluted with H_2O (10 mL), extracted with CH_2Cl_2 (3 x 10 mL), then the combined organics were dried (Na_2SO_4), filtered, and concentrated *in vacuo* to give the desired product as a yellow solid (69 mg, 84%).

^{1}H NMR (300 MHz, $CDCl_3$): δ 8.25 (1H, d, *J* = 9.1 Hz), 7.15 (1H, d, *J* = 9.1 Hz).

The data observed is in accordance with literature values.[2]

4-Azidoaniline

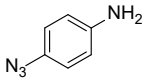

4-Aminophenylboronic acid HCl (87 mg, 0.50 mmol) was dissolved in MeOH (2.5 mL), under air. NaN_3 (49 mg, 0.75 mmol) and $Cu(OAc)_2$ (10 mg, 0.05 mmol) were added and the reaction mixture was heated to 55 °C and stirred for 16 h. The reaction mixture was then diluted with H_2O (10 mL), extracted with CH_2Cl_2 (3 x 10 mL), then the combined organics were dried (Na_2SO_4), filtered, and concentrated *in vacuo*, to give the desired product as a brown oil (42 mg, 63%).

^{1}H NMR (300 MHz, $CDCl_3$): δ 6.85 (1H, d, *J* = 8.7 Hz), 6.68 (1H, d, *J* = 8.7 Hz), 3.65 (2H, br. s).

The data observed is in accordance with literature values.[2]

***N*-Butyl-4-butylamino-6-(1-(4-nitrophenyl)-1,2,3-triazol-4-yl)-1,8-naphthalimide**

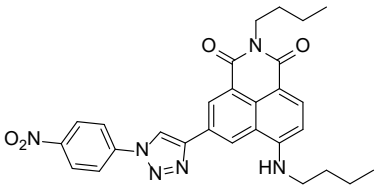

3NO$_2$

N-Butyl-4-butylamino-6-ethynyl-1,8-naphthalimide (42 mg, 0.12 mmol), 1-azido-4-nitrobenzene (23 mg, 0.14 mmol), $CuSO_4.5H_2O$ (1.5 mg, 5 mol%), NaAsc (4.8 mg, 20 mol%), and Na_2CO_3 (21 mg, 0.20 mmol) were dissolved in THF:H_2O (5:1, 3 mL) under a nitrogen atmosphere. The resultant mixture was stirred for 16 h, then diluted with H_2O (10 mL), extracted with CH_2Cl_2 (3 x 10 mL), dried (Na_2SO_4), filtered, and concentrated *in vacuo*. Purification *via* automated flash chromatography (silica gel, 0 – 25% EtOAc in hexanes) gave the desired product as a yellow solid (41 mg, 66%).

^{1}H NMR (500 MHz, $CDCl_3$): δ 9.00 (1H, d, *J* = 1.1 Hz), 8.81 (1H, d, *J* = 1.1 Hz), 8.60 (1H, s), 8.49 (2H, d, *J* = 9.0 Hz), 8.46 (1H, d, *J* = 8.4 Hz), 8.08 (2H, d, *J* = 9.0 Hz), 6.81 (1H, d, *J* = 8.3 Hz), 4.20 - 4.17 (2H, m), 3.47

(2H, t, *J* = 7.3 Hz), 1.89 - 1.83 (2H, m), 1.76 - 1.70 (2H, m), 1.60 - 1.53 (2H, m), 1.50 - 1.43 (2H, m), 1.05 (3H, t, *J* = 7.4 Hz), 0.99 (3H, t, *J* = 7.4 Hz).

^{13}C NMR (125 MHz, $CDCl_3$): δ 163.5, 162.9, 149.0, 147.1, 146.5, 139.9, 134.0, 128.7, 127.1, 124.7, 124.6, 122.9, 121.7, 119.6, 119.5, 117.0, 109.0, 103.9, 42.6, 39.1, 30.0, 29.3, 28.7, 19.4, 12.9, 12.8.

HRMS (ESI): calculated for $C_{28}H_{29}N_6O_4$ $[M+H]^+$ m/z 513.2245, observed 513.2244.

***N*-Butyl-4-butylamino-6-(1-(4-aminophenyl)-1,2,3-triazol-4-yl)-1,8-naphthalimide**

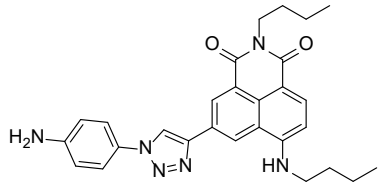

$3NH_2$

N-Butyl-4-butylamino-6-ethynyl-1,8-naphthalimide (42 mg, 0.12 mmol), 4-azidoaniline (19 mg, 0.14 mmol), $CuSO_4.5H_2O$ (1.5 mg, 5 mol%), NaAsc (4.8 mg, 20 mol%), and Na_2CO_3 (21 mg, 0.20 mmol) were dissolved in THF:H_2O (5:1, 3 mL) under a nitrogen atmosphere. The resultant mixture was stirred for 16 h, then diluted with H_2O (10 mL), extracted with CH_2Cl_2 (3 x 10 mL), dried (Na_2SO_4), filtered, and concentrated *in vacuo*. Purification *via* automated flash chromatography (silica gel, 15 - 50% EtOAc in hexanes) gave the desired product as an orange solid (57 mg, 98%).

^{1}H NMR (500 MHz, $CDCl_3$): δ 8.98 (1H, s), 8.78 (1H, d, *J* = 1.2 Hz), 8.45 (1H, d, *J* = 8.4 Hz), 8.31 (1H, s), 7.56 (2H, d, *J* = 8.6 Hz), 6.83 (2H, d, *J* = 8.6 Hz), 6.74 (1H, d, *J* = 8.4 Hz), 5.65 (1H, br s), 4.20 - 4.17 (2H, m), 3.46 - 3.42 (2H, m), 1.86 - 1.80 (2H, m), 1.75 - 1.68 (2H, m), 1.59 - 1.53 (2H, m), 1.49 - 1.43 (2H, m), 1.04 (3H, t, *J* = 7.4 Hz), 0.98 (3H, t, *J* = 7.4 Hz).

^{13}C NMR (125 MHz, $CDCl_3$): δ 164.8, 164.2, 150.1, 147.5, 147.0, 134.8, 129.6, 128.6, 128.5, 126.9, 123.9, 122.5, 122.4, 120.8, 118.7, 115.6, 110.1, 104.8, 43.7, 40.2, 31.1, 30.5, 20.6, 20.6, 14.0, 14.0.

HRMS (ESI): calculated for $C_{28}H_{31}N_6O_2$ $[M+H]^+$ m/z 483.2503, observed 483.2502.

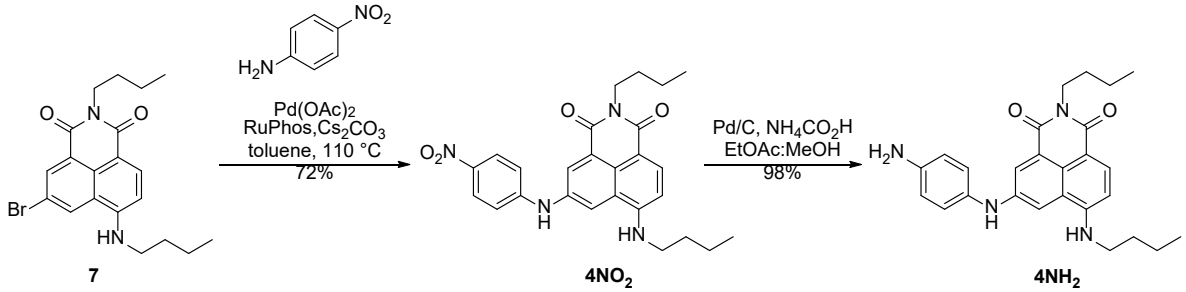

7 **$4NO_2$** **$4NH_2$**

Scheme S5: Synthesis of **$4NO_2$** and **$4NH_2$**.

***N*-Butyl-4-butylamino-6-((4-nitrophenyl)amino)-1,8-naphthalimide**

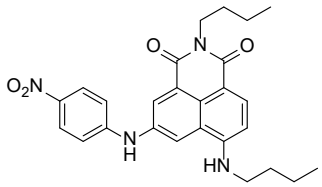

4NO$_2$

N-Butyl-3-bromo-5-butylamino-1,8-naphthalimide (80 mg, 0.24 mmol) 4-nitroaniline (38 mg, 0.28), and Cs_2CO_3 (118 mg, 0.36 mmol) were dissolved in toluene (10 mL) and the resultant mixture was degassed *via* freeze-pump-thaw. $Pd(OAc)_2$ (2.8 mg, 5 mol%) and RuPhos (5.6 mg, 5 mol%) were added and the reaction mixture heated to reflux and stirred for 4 h. The reaction mixture was then diluted with EtOAc (30 mL), washed with H_2O (30 mL), brine (30 mL), and dried (Na_2SO_4), filtered, and concentrated *in vacuo*. Purification *via* automated flash chromatography (silica gel, 0-30% EtOAc in hexanes) gave the desired product as a bright red solid (80 mg, 72%).

^{1}H NMR (500 MHz, $CDCl_3$): δ 8.43 (1H, d, *J* = 2.0 Hz), 8.41 (1H, d, *J* = 8.4 Hz), 8.15 (2H, d, *J* = 9.1 Hz), 7.89 (1H, d. *J* = 2.0 Hz), 7.02 (2H, d, *J* = 9.1 Hz), 6.74 (1H, d, *J* = 8.4 Hz), 6.64 (1H, d, *J* = 2.0 Hz), 5.12 (1H, t, *J* = 5.1 Hz), 4.17 - 4.14 (2H, m), 3.43 - 3.39 (2H, m), 1.82 - 1.76 (2H, m), 1.74 - 1.68 (2H, m), 1.57 - 1.49 (2H, m), 1.48 - 1.41 (2H, m), 1.02 (3H, t, *J* = 7.4 Hz), 0.98 (3H, t, *J* = 7.4 Hz).

^{13}C NMR (125 MHz, $CDCl_3$): δ 164.1, 163.9, 149.6, 148.6, 140.6, 136.9, 133.6, 127.1, 126.4, 125.1, 121.4, 117.3, 114.1, 110.5, 105.0, 43.6, 40.1, 31.0, 30.3, 20.4, 20.4, 13.9, 13.9.

HRMS (APPI): calculated for $C_{22}H_{20}N_2O_2$ $[M]^+$ m/z 460.2105, observed 460.2106.

***N*-Butyl-4-butylamino-6-((4-aminophenyl)amino)-1,8-naphthalimide**

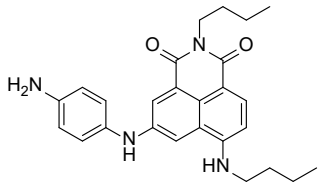

4NH$_2$

N-Butyl-4-butylamino-6-((4-nitrophenyl)amino)-1,8-naphthalimide (40 mg, 0.09 mmol) was dissolved in EtOAc:MeOH (5:1, 5 mL), under a nitrogen atmosphere. Pd/C (10 mg) was added, followed by NH_4HCO_2 (28 mg, 0.45 mmol) and the resultant mixture was stirred for 16 h. The reaction mixture was filtered through a pad of celite, washed thoroughly with EtOAc, and then concentrated *in vacuo*, to give the desired product as a dark red solid (38 mg, 98%).

^{1}H NMR (500 MHz, $CDCl_3$): δ 8.23 (1H, d, *J* = 8.3 Hz), 8.14 (1H, d, *J* = 1.8 Hz), 7.34 (1H, d, *J* = 1.8 Hz), 7.05 (2H, d, *J* = 8.4 Hz), 6.72 (2H, d. *J* = 8.4 Hz), 6.62 (1H, d, *J* = 8.3 Hz), 5.85 (1H, s), 4.85 (1H, s), 4.14 - 4.11 (2H, m), 3.37 - 3.32 (2H, m), 1.76 - 1.66 (4H, m), 1.52 - 1.39 (4H, m), 1.00 (3H, t, *J* = 7.4 Hz), 0.96 (3H, t, *J* = 7.3 Hz).

^{13}C NMR (125 MHz, $CDCl_3$): δ 164.7, 164.3, 147.8, 143.9, 143.3, 132.5, 130.9, 124.4, 124.2, 124.0, 121.9, 121.6, 116.3, 110.6, 106.9, 104.4, 43.4, 40.0, 31.0, 30.3, 20.4, 20.3, 13.9, 13.9.

HRMS (ESI): calculated for $C_{26}H_{31}N_4O_2$ $[M+H]^+$ m/z 431.2442, observed 431.2442.

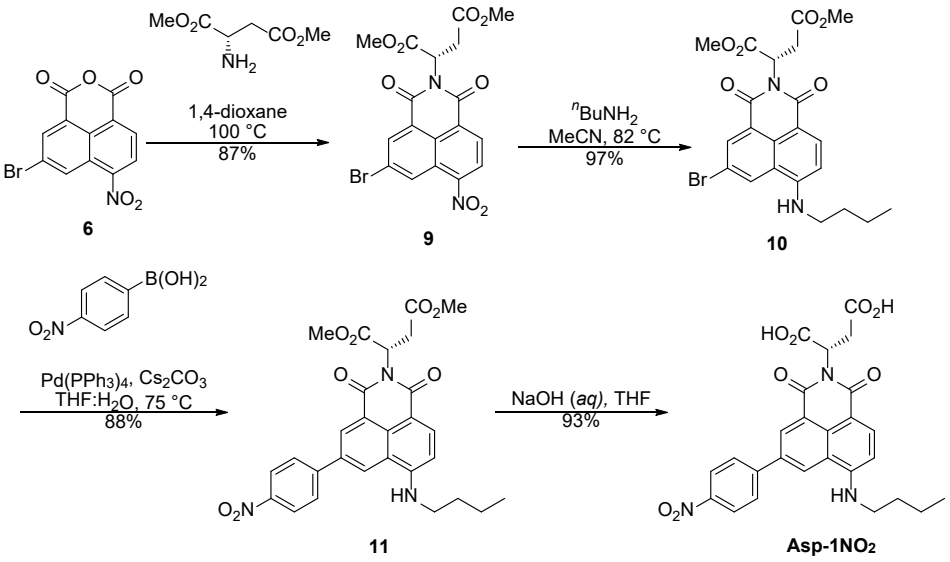

Scheme 6: Synthesis of **Asp-1NO$_2$**.

L-Aspartic acid dimethyl ester

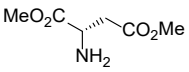

L-Aspartic acid (2.00 g, 15.0 mmol) was suspended in MeOH (30 mL) under a nitrogen atmosphere. Conc. H_2SO_4 (0.5 mL) was added and the resultant solution was heated to 65 °C and stirred for 16 h. The reaction mixture was then diluted with H_2O (100 mL), pH adjusted to pH 10 using 2M NaOH (*aq*), then extracted with CH_2Cl_2 (3 x 75 mL). The combined organics were dried (Na_2SO_4), filtered, and concentrated *in vacuo*, to give the desired product as a pale yellow oil (458 mg, 19%).

^{1}H NMR (300 MHz, $CDCl_3$): δ 3.84 (1H, dd, *J* = 7.2, 4.8 Hz), 3.75 (3H, s), 3.71 (3H, s), 2.83 (1H, dd, *J* = 16.5, 4.8 Hz), 2.72 (1H, dd, *J* = 16.5, 7.2 Hz).

The data observed is in accordance with literature values.[3]

N-Dimethyl succinate-3-bromo-5-nitro-1,8-naphthalimide

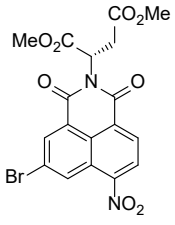

9

3-Bromo-5-nitro-1,8-naphthalic anhydride (300 mg, 0.94 mmol) and L-aspartic acid dimethyl ester (166 mg, 1.03 mmol) were dissolved in 1,4-dioxane (10 mL), under a nitrogen atmosphere and the resultant mixture was heated to reflux and stirred for 16 h. The reaction mixture was then cooled, diluted with EtOAc (30 mL), washed with H2O (30 mL), and brine (30 mL). The organic phase was dried

(Na_2SO_4), filtered, and concentrated *in vacuo* to give the desired product as a yellow solid (379 mg, 87%).

^{1}H NMR (500 MHz, $CDCl_3$): δ 9.10 (1H, d, J = 1.8 Hz), 8.82 (1H, d, J = 1.8 Hz), 8.71 (1H, d, J = 8.0 Hz), 8.48 (1H, d, J = 8.0 Hz), 6.21 (1H, dd, J = 8.0, 6.2 Hz), 3.76 (3H, s), 3.67 (3H, s), 3.51 (1H, dd, J = 16.8, 6.2 Hz), 3.05 (1H, dd, J = 16.8, 6.2 Hz).

^{13}C NMR (125 MHz, $CDCl_3$): δ 170.7, 168.7, 161.8, 161.6, 148.5, 136.2, 131.9, 130.5, 127.8, 126.7, 125.3, 125.1, 124.9, 123.8, 53.1, 52.1, 50.1, 33.7.

HRMS (ESI): calculated for $C_{18}H_{14}N_2O_8Br$ [M]+ m/z 464.9928, observed 464.9929.

***N*-Dimethyl succinate-3-bromo-5-butylamino-nitro-1,8-naphthalimide**

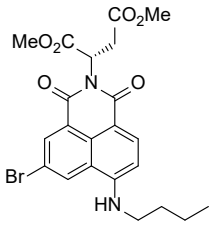

10

N-dimethyl succinate-3-bromo-5-nitro-1,8-naphthalimide (150 mg, 0.34 mmol) was dissolved in anhydrous MeCN (10 mL) under a nitrogen atmosphere. ^{n}BuNH$_2$ (300 µL, 3.03 mmol) was added and the reaction mixture heated to reflux and stirred for 16 h. The reaction mixture was then diluted with CH_2Cl_2 (100 mL), washed with 0.5 M (*aq*) HCl (100 mL), the aqueous extracted with CH_2Cl_2 (2 x 50 mL), and the combined organic extracts dried (Na_2SO_4), filtered, and concentrated *in vacuo*. Purification *via* automated flash chromatography (silica gel, 10 - 30% EtOAc in hexanes) gave the desired product as a bright red solid (153 mg, 97%).

^{1}H NMR (500 MHz, $CDCl_3$): δ 8.40 (1H, d, *J* = 1.8 Hz), 8.34 (1H, d, *J* = 8.5 Hz), 8.12 (1H, d, *J* = 1.8 Hz), 6.59 (1H, d, *J* = 8.5 Hz), 6.23 (1H, dd, *J* = 7.4, 6.5 Hz), 5.72 (1H, t, *J* = 5.0 Hz), 3.78 (3H, s), 3.72 (3H, s), 3.53 (1H, dd, *J* = 16.4, 6.5 Hz), 3.37 - 3.33 (2H, m), 3.03 (1H, dd, *J* = 16.4, 7.4 Hz), 1.80 - 1.74 (2H, m), 1.56 - 1.48 (2H, m), 1.03 (3H, t, *J* = 7.4 Hz).

^{13}C NMR (125 MHz, $CDCl_3$): δ 171.5, 170.1, 162.9, 162.8, 149.2, 135.3, 133.9, 129.1, 128.3, 123.5, 121.2, 118.3, 108.6, 104.9, 52.9, 52.1, 49.6, 43.5, 34.2, 30.7, 20.3, 13.8.

HRMS (APPI): calculated for $C_{22}H_{23}N_2O_6Br$ $[M]^+$ m/z 490.0734, observed 490.0734.

***N*-Dimethyl succinate-4-butylamino-6-(4-nitrophenyl)-1,8-naphthalimide**

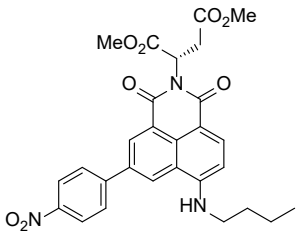

11

N-Dimethyl succinate-3-bromo-5-butylamino-nitro-1,8-naphthalimide (59 mg, 0.12 mmol), 4-nitrophenylboronic acid (25 mg, 0.15 mmol), $Pd(PPh_3)_4$ (14 mg, 10 mol%), and Cs_2CO_3 (117 mg, 0.36 mmol) were dissolved in thoroughly degassed THF:H_2O (5:1, 5 mL) under a nitrogen atmosphere. The resultant solution was heated to 75 °C and stirred for 16 h. The reaction mixture was then filtered through celite, washed with EtOAc (100 mL), and concentrated *in vacuo*. Purification *via* flash chromatography (silica gel 0 - 35% EtOAc in hexanes) gave the desired product as an orange solid (56 mg, 88%).

^{1}H NMR (500 MHz, $CDCl_3$): δ 8.57 (1H, s), 8.36 (2H, dd, *J* = 8.6 Hz), 8.26 (1H, d, *J* = 1.1 Hz), 8.22 (1H, d, *J* = 8.5 Hz), 7.83 (2H, d, *J* = 8.6 Hz), 6.57 (1H, d, *J* = 8.5 Hz), 6.27 (1H, t, *J* = 6.9 Hz), 6.06 (1H, t, *J* = 4.5 Hz), 3.85 (3H, s), 3.70 (3H, s), 3.55 (1H, dd, *J* = 16.4, 6.7 Hz), 3.43 - 3.38 (2H, m), 2.95 (1H, dd, *J* = 16.4, 7.1 Hz), 1.82 - 1.75 (2H, m), 1.58 - 1.48 (2H, m), 1.03 (3H, t, *J* = 7.3 Hz).

^{13}C NMR (125 MHz, $CDCl_3$): δ 171.3, 170.6, 163.7, 162.9, 150.6, 147.5, 145.7, 135.5, 134.8, 130.1, 129.6, 128.1, 125.2, 124.3, 122.8, 120.3, 108.4, 104.9, 53.0, 52.0, 49.7, 43.6, 34.3, 30.7, 20.3, 13.8.

HRMS (APCI): calculated for $C_{28}H_{27}N_3O_8$ $[M+H]^+$ m/z 534.1876, observed 534.1873.

Asp-1NO$_2$

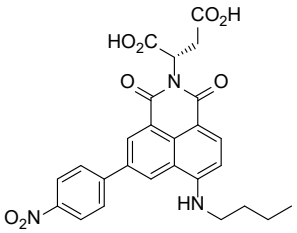

Asp-1NO$_2$

N-Dimethyl succinate-4-butylamino-6-(4-nitrophenyl)-1,8-naphthalimide (40 mg, 0.07 mmol) was dissolved in THF (3 mL), under a nitrogen atmosphere. 2M NaOH (*aq*) (1 mL) was added and the resultant mixture stirred for 24 h. The reaction mixture was then diluted with H_2O (25 mL) and extracted with CH_2Cl_2 (25 mL). The aqueous was then acidified to pH <2 with 2M HCl (*aq*) and extracted with 10% ^{i}PrOH in $CHCl_3$ (4 x 25 mL), dried (Na_2SO_4), filtered, and concentrated *in vacuo*. Purification *via* flash chromatography (silica gel 0 - 5% MeOH in CH_2Cl_2 with 0.1% AcOH) to give the desired product as an orange solid (33 mg, 93%).

^{1}H NMR (500 MHz, $CDCl_3$): δ 9.15 (1H, s), 8.76 (1H, s), 8.41 (2H, d, *J* = 8.7 Hz), 8.30 (1H, d, *J* = 8.6 Hz), 8.22 (2H, d, *J* = 8.7 Hz), 8.15 (1H, t, *J* = 5.3 Hz), 6.87 (1H, d, *J* = 8.8 Hz), 5.93 (1H, br. s), 3.48 – 3.42 (2H, m), 3.39 – 3.33 (2H, m)*, 2.73 – 2.53 (2H, m), 1.78 – 1.68 (2H, m), 1.52 – 1.40 (2H, m), 0.97 (3H, t, *J* = 7.3 Hz).

^{13}C NMR (125 MHz, DMSO-d_6): δ 173.0, 171.7, 163.9, 162.9, 152.0, 147.6, 145.9, 135.8, 134.3, 130.1, 129.9, 128.9, 128.1, 124.9, 123.2, 121.2, 107.5, 105.3, 49.9, 43.3, 31.3, 30.7, 20.5, 14.4.

HRMS (ESI): calculated for $C_{26}H_{23}N_3O_8Na$ $[M+Na]^+$ m/z 528.1377, observed 528.1377.

*obscured by residual H_2O

Spectroscopic materials and methods

The solvents used in all photophysical studies were CH_2Cl_2 (HPLC grade, Sigma Aldrich), absolute EtOH (200 proof, HPLC/spectrophotometric grade, Sigma Aldrich) or HEPES buffer (Millipore water, 100 mM, pH 7.4). Stock solutions were prepared in DMSO (Spectroscopy grade, Sigma Aldrich) and samples prepared by dilution of the stock to the required concentration (DMSO <0.05 %v/v).

Absorption spectra were obtained in CH_2Cl_2 (10 µM) on a Varian Cary 400 UV-Vis spectrophotometer using 10 mm quartz cuvettes.

Excitation and emission spectra were measured at 1 µM and 5 µM in CH_2Cl_2; 5 µM in EtOH; and 50 µM in HEPES buffer on a Varian Cary Eclipse fluorometer using quartz cuvettes.

Absolute quantum yields were measured at 2.5 µM in spectroscopic grade absolute EtOH on a PTI QuantaMaster 400 fluorometer with an integrating sphere in 3.5 mL quartz cuvettes. Samples were prepared in triplicate and the mean reported.

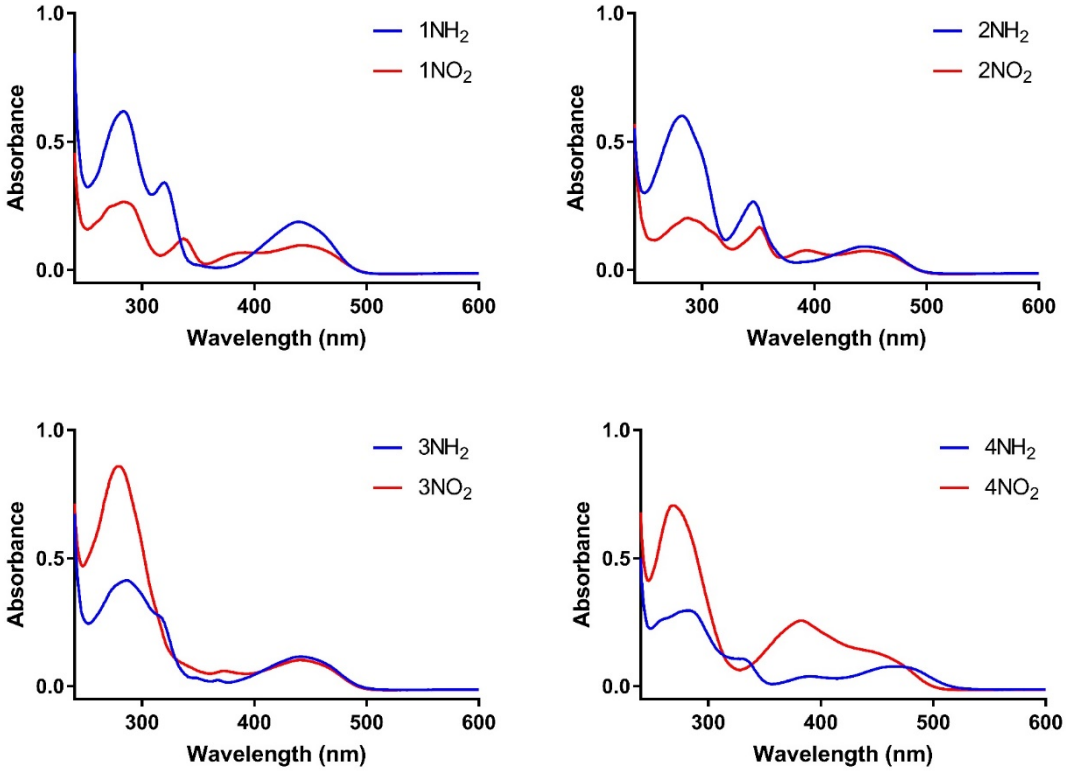

Figure S1: UV/Vis absorbance spectra of **1** – **4** (2.5 µM in CH_2Cl_2).

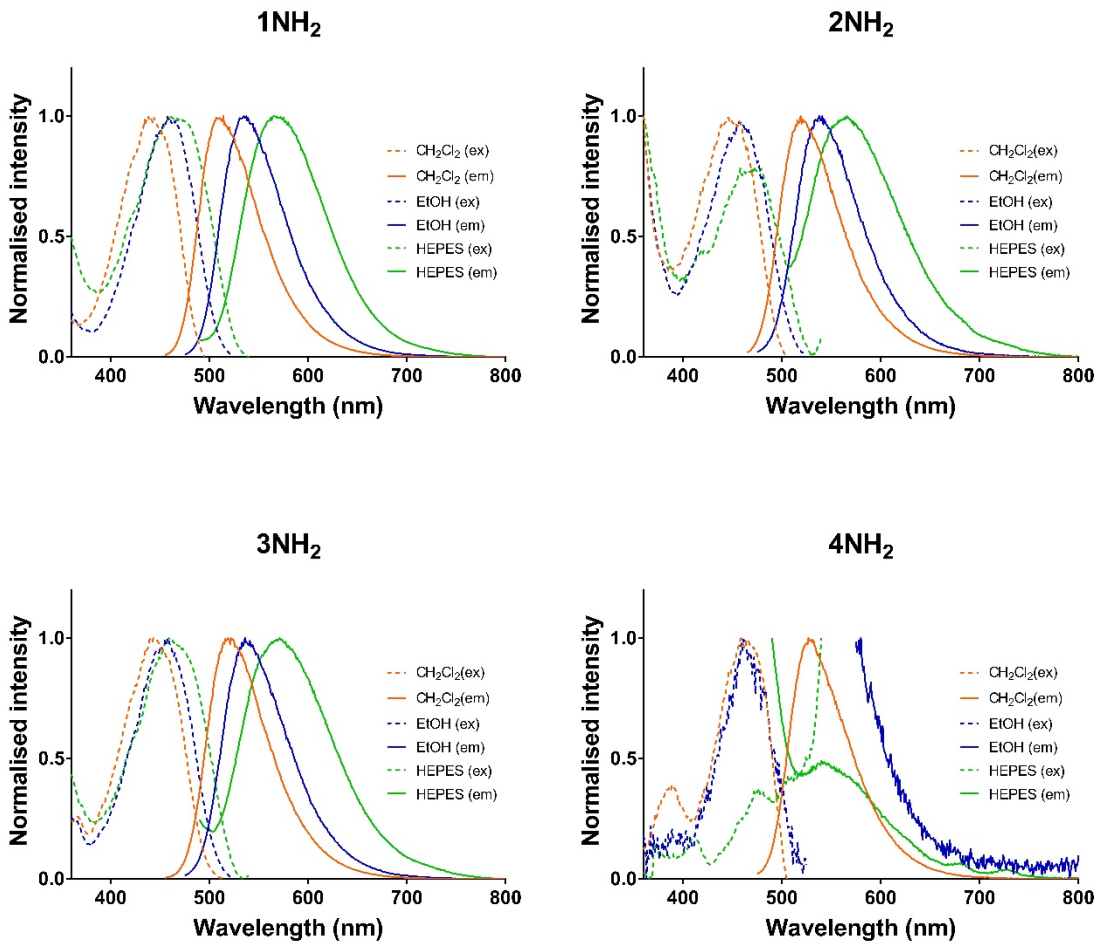

Figure S2: Excitation and emission spectra of **$1NH_2$** – **$4NH_2$** (5 µM CH_2Cl_2, 5 µM EtOH, 50 µM HEPES buffer 100 mM pH 7.4).

Table S1: Comparison of absolute quantum yield (in EtOH) of **$1NO_2$** – **$4NO_2$**, **$1NH_2$** – **$4NH_2$**, and unsubstituted N-Butyl-4-butylamino-1,8-naphthalimide.

	Φ	
	NO_2	**NH_2**
1	<0.01	0.42
2	<0.01	0.06
3	0.06	0.16
4	<0.01	0.02
Unsubstituted	0.63	

Theoretical Methods

To model the excited state spectra of the dyes, we have applied a protocol used extensively in the Nantes' group. The total and transition energies are determined with second-order Coupled-Cluster calculations (CC2), whereas the geometries, vibrations, and environmental effects are computed at the Time-Dependent Density Functional Theory (TD-DFT) level. All CC2 calculations were achieved with TURBOMOLE,[4] applying the resolution-of-identity approach (RI-V) and selecting the *aug*-cc-pVDZ atomic basis set. All (TD-)DFT calculations have been performed using the Gaussian16.A03 program.[5] For these Gaussian calculations, we used tightened self-consistent field (10^{-10} a.u.) and geometry optimization (10^{-5} a.u.) convergence thresholds, and a large DFT integration grid (so-called *ultrafine* grid, a pruned (99,590) grid). These (TD-)DFT calculations relied on the hybrid M06-2X functional.[6] Following the basis set combination approach,[7] we used the 6-311G(d,p) atomic basis set for determining the geometrical and vibrational parameters whereas the transition energies have been computed with 6-311++G(d,p). The nature of the ground-state stationary points was confirmed by analytical Hessian calculations that returned 0 (minima) imaginary vibrational modes. Environmental effects (here, dichloromethane) on the transition energies have been accounted for using the polarizable continuum model (PCM).[8] For the geometrical and vibrational calculations, we did use the standard LR (linear-response) PCM model in its *equilibrium* limit, which is the default in Gaussian16. For both absorption and emission, we used a more refined LR+cLR[9] model in its *non-equilibrium* limit, to capture both linear-response and state-specific solvent effects. For the ISC estimates, we have determined singlet and triplet energies on the lowest S_1 geometry using the TDA approximation of TD-DFT and the same functional and basis set as above. It is known that TDA generally provides more accurate S-T gaps than "full" TD-DFT. Excited-states have been represented using density difference plots, in which the excited-state density was determined at the TD-DFT level. In these plots blue and red regions respectively indicate decrease and increase of electron density upon photon absorption (a contour threshold of $8\ 10^{-4}$ au is used in all representations).

Biological studies

Cell culture

DLD-1 human colon carcinoma cells were maintained in exponential growth as monolayers in Advanced Dulbecco's Modified Eagle Medium (DMEM), supplemented with 2% foetal bovine serum (FBS), and 1% glutamine at 37 ˚C in 5% CO_2.

Preparation of cells for spheroid imaging experiments

Trypsin was added to DLD-1 colon carcinoma cells when 50% confluent and the cells were mixed thoroughly to break up clumps. Cells were seeded at 20,000, 10,000, 5,000, and 2,500 cells per well in a 96 well plate (Costar® ultra-low cluster, ultra-low attachment, polystyrene, non-polystyrene) and were left to grow over 3 days. Stock solutions of probe in media was added in quadruplicate to give a final concentration of 50 μM and the spheroids were incubated for 20 h. The spheroids were collected and washed twice with PBS and then were transferred to a MatTek 35 mm glass-bottom dish in FluoroBrite™ media supplemented with 2% FBS for imaging.

Leica SP5 live spheroid imaging

Confocal microscopy images were acquired using a Leica SP5 II confocal and multi-photon microscope with a 10X dry objective lens. Excitation light of 496 nm was provided by an argon laser. Images were

collected using the Leica Application Suite Advanced Fluorescence lite Version 2.8.0 build 7266 viewer software and image processing was performed using Fiji/ImageJ (version 2.0.0).

Cytotoxicity

DLD-1 cells were seeded at 7,500 cells per well in a 96 well plate. The cells were left to adhere overnight, then a stock solution of probe in media was added in triplicate to give a final concentration of 200, 100 and 50 µM. The cells were incubated for 24 h, then 10 µL of alamarBlue (ThermoFischer) solution was added to each well and left to incubate for a further 2 h. The reduction of alamarBlue was measured by fluorescence (λ_{ex} = 570 nm, λ_{em} = 585 nm). The percentage cell viability was calculated relative to control wells.

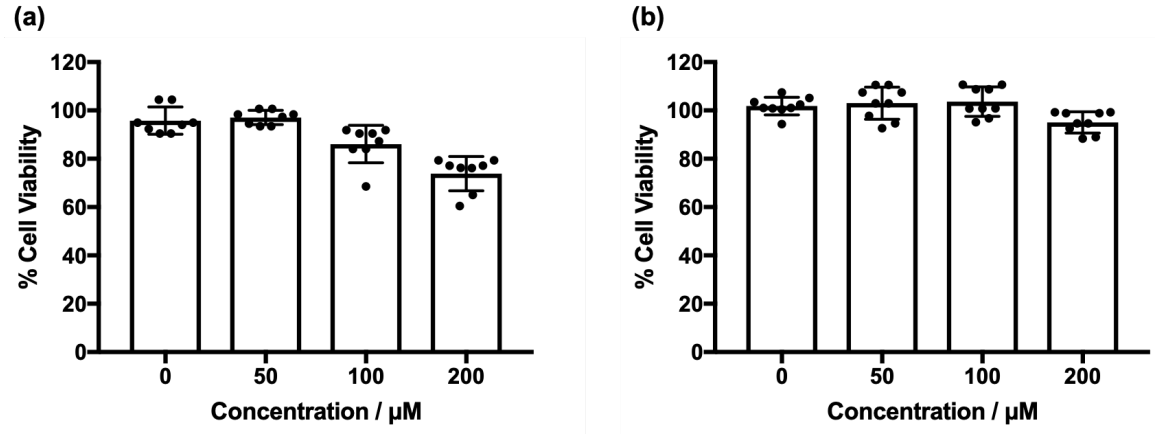

Figure S3: (a) Cell viability of DLD-1 cells after treatment with probe **1NO$_2$** for 24 h at varying concentrations (b) cell viability of DLD-1 cells after treatment with probe **Asp-1NO$_2$** for 24 h at varying concentrations. Data are represented as the mean ± SEM from three independent experiments.

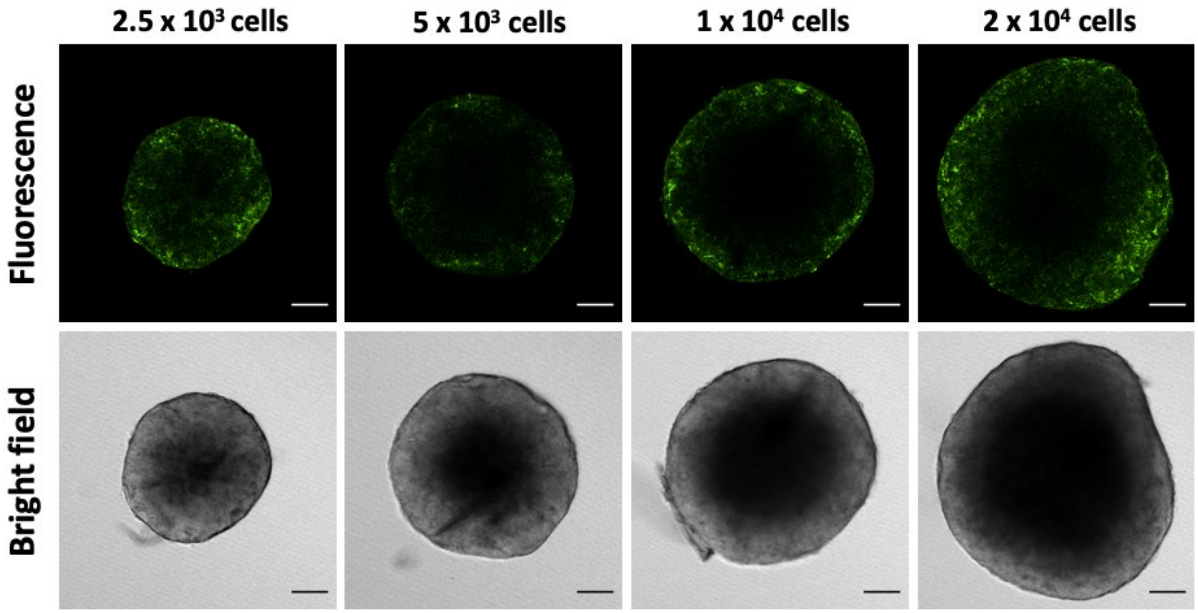

Figure S4: Confocal microscopy images of DLD-1 spheroids of varying sizes treated with 20 µM of **1NO$_2$** (scale bar represents 100 µm).

NMR Spectra

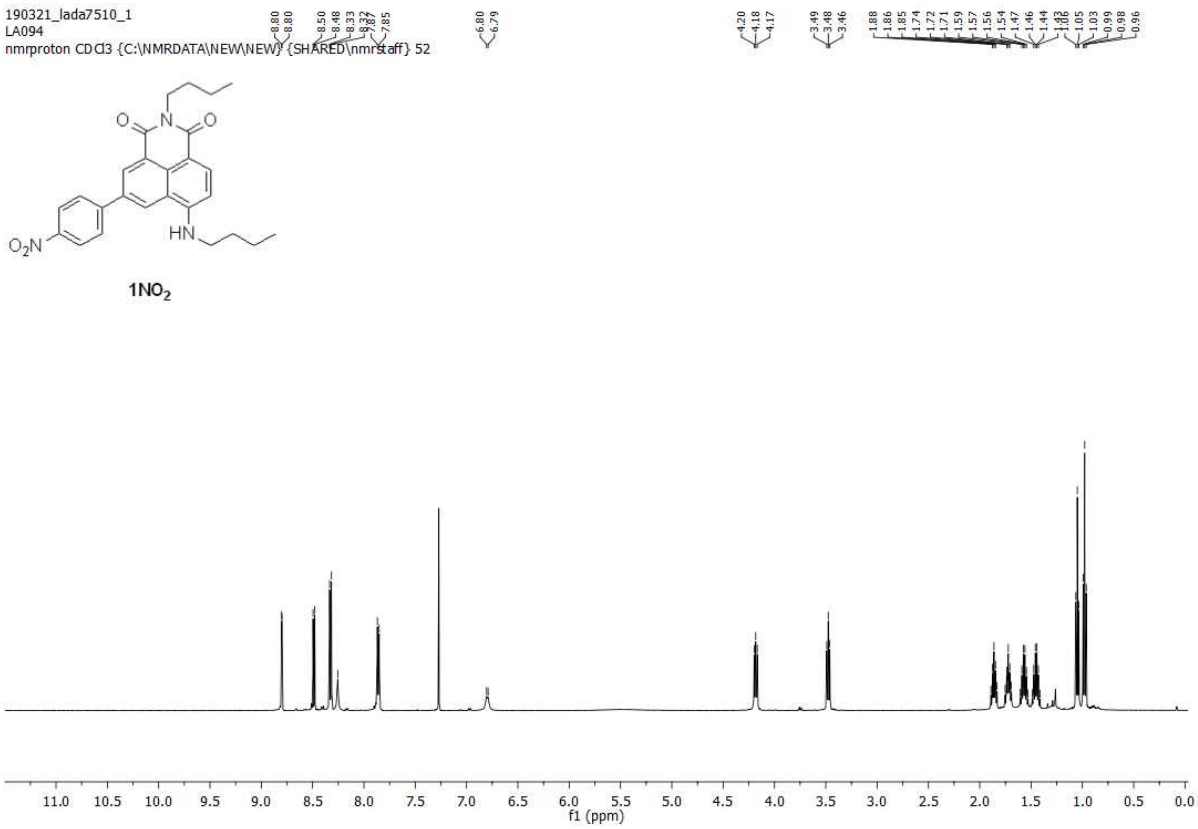

$1NO_2$

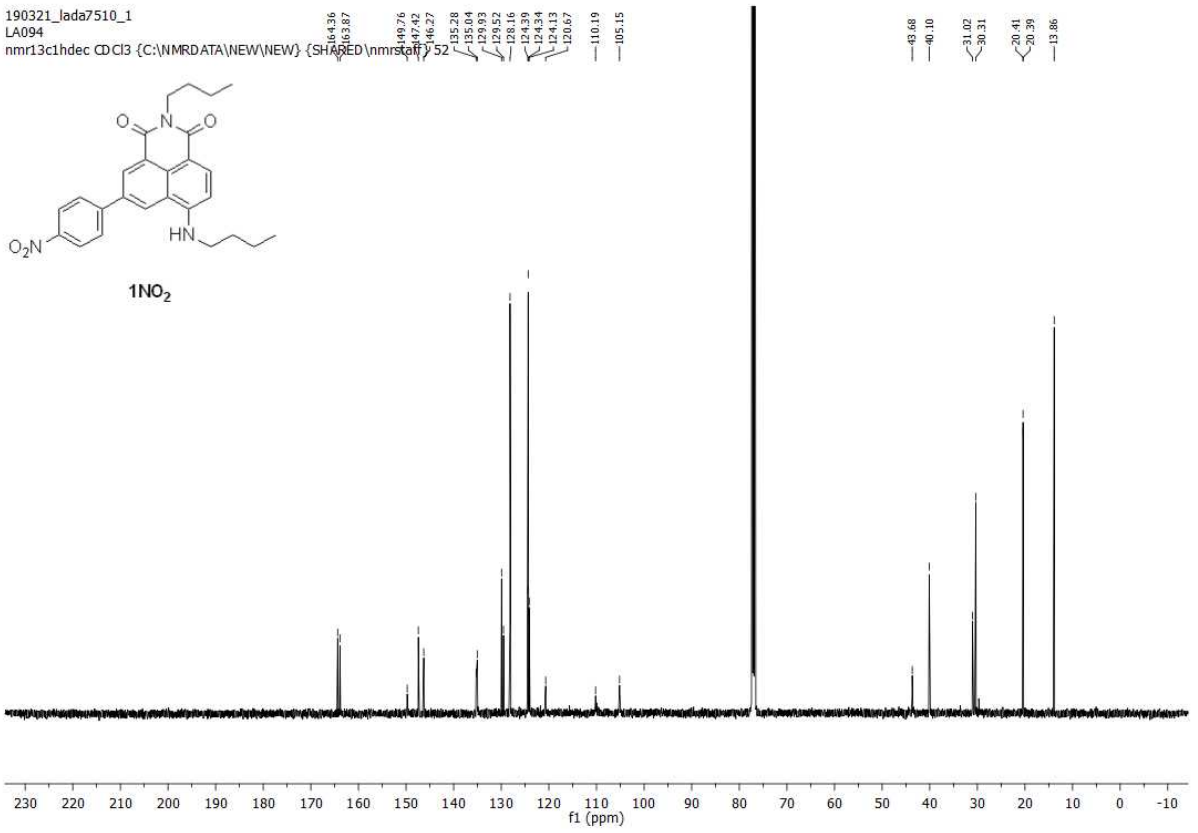

$1NO_2$

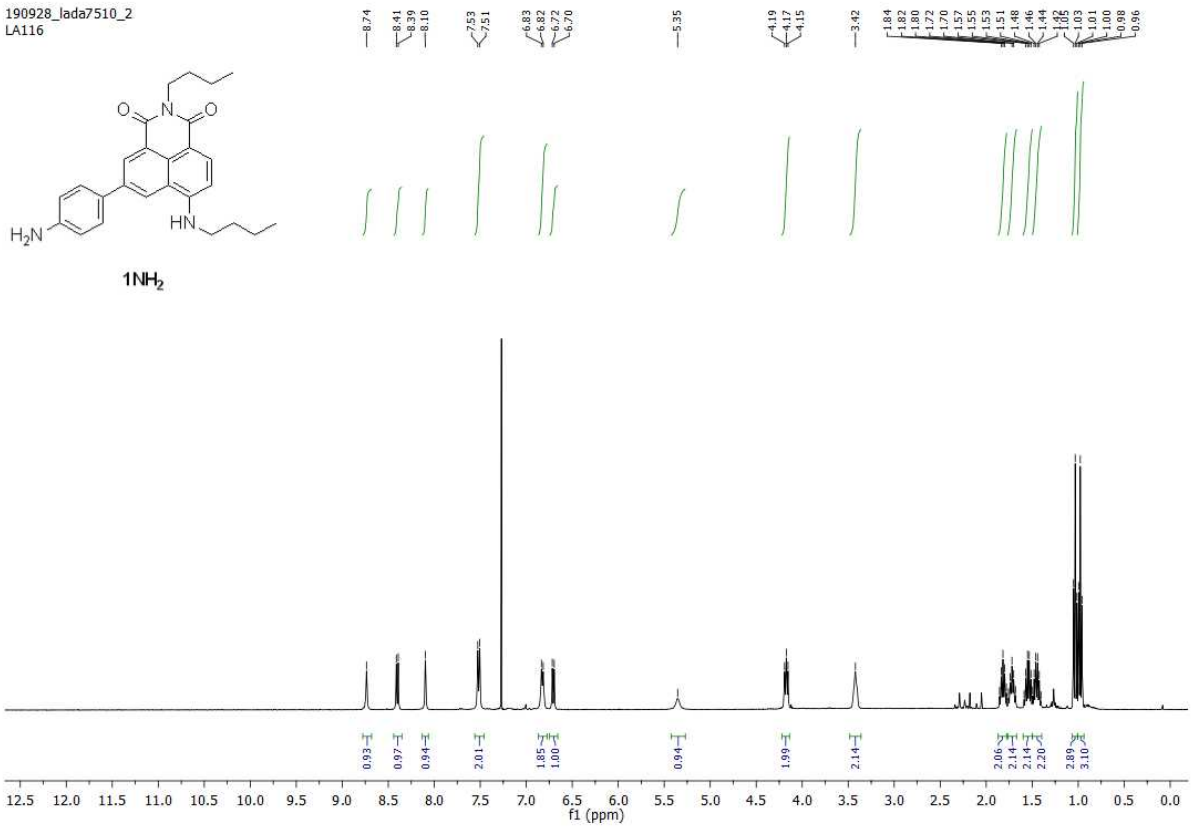
190928_lada7510_2
LA116
8.74
8.41
8.39
8.10
7.53
7.51
6.83
6.82
6.72
6.70
5.35
4.19
4.17
4.15
3.42
1.84
1.82
1.80
1.72
1.70
1.57
1.55
1.53
1.51
1.48
1.46
1.44
1.42
1.05
1.03
1.01
1.00
0.98
0.96
O
N
O
HN
H_2N
0.93
0.97
0.94
2.01
1.85
1.00
0.94
1.99
2.14
2.06
2.14
2.14
2.20
2.89
3.10
12.5 12.0 11.5 11.0 10.5 10.0 9.5 9.0 8.5 8.0 7.5 7.0 6.5 6.0 5.5 5.0 4.5 4.0 3.5 3.0 2.5 2.0 1.5 1.0 0.5 0.0
f1 (ppm)

1NH$_2$

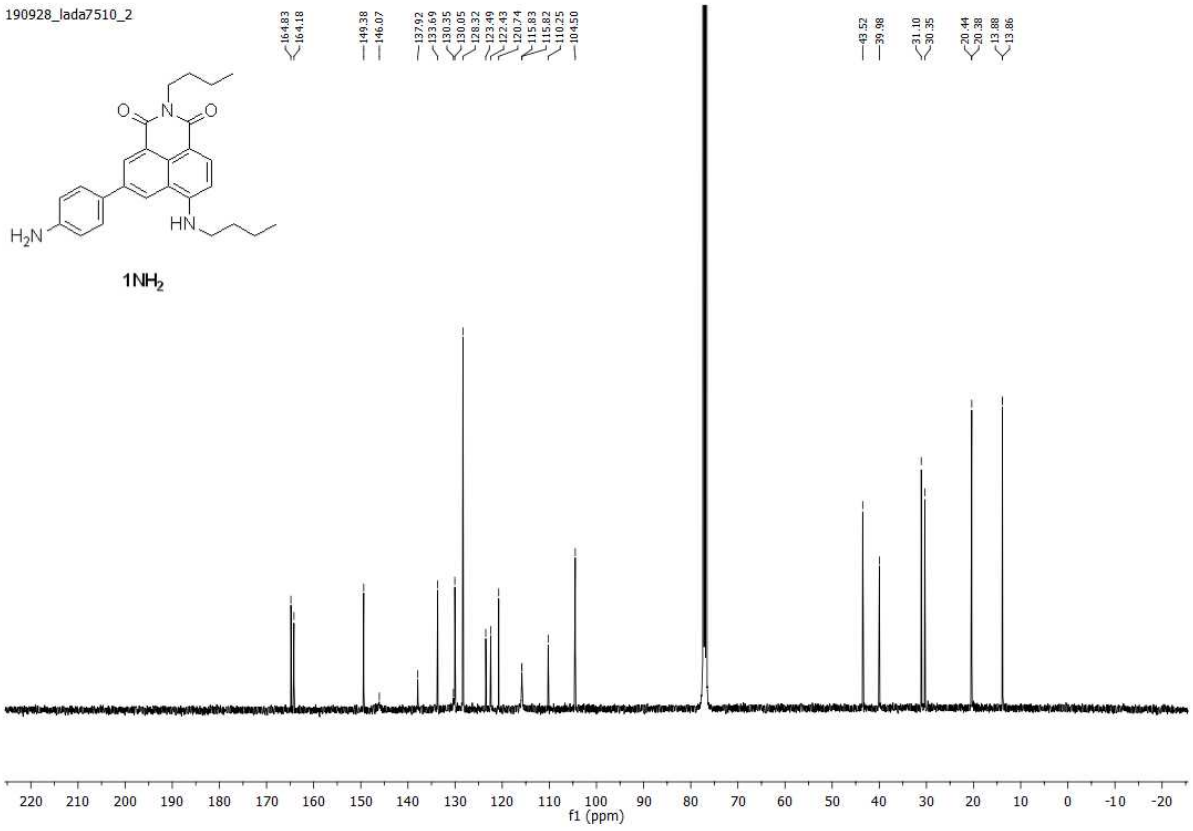
190928_lada7510_2
164.83
164.18
149.38
146.07
137.92
133.69
130.35
130.05
128.32
123.49
122.43
120.74
115.83
115.82
110.25
104.50
43.52
39.98
31.10
30.35
20.44
20.38
13.88
13.86
O
N
O
HN
H_2N
220 210 200 190 180 170 160 150 140 130 120 110 100 90 80 70 60 50 40 30 20 10 0 -10 -20
f1 (ppm)

1NH$_2$

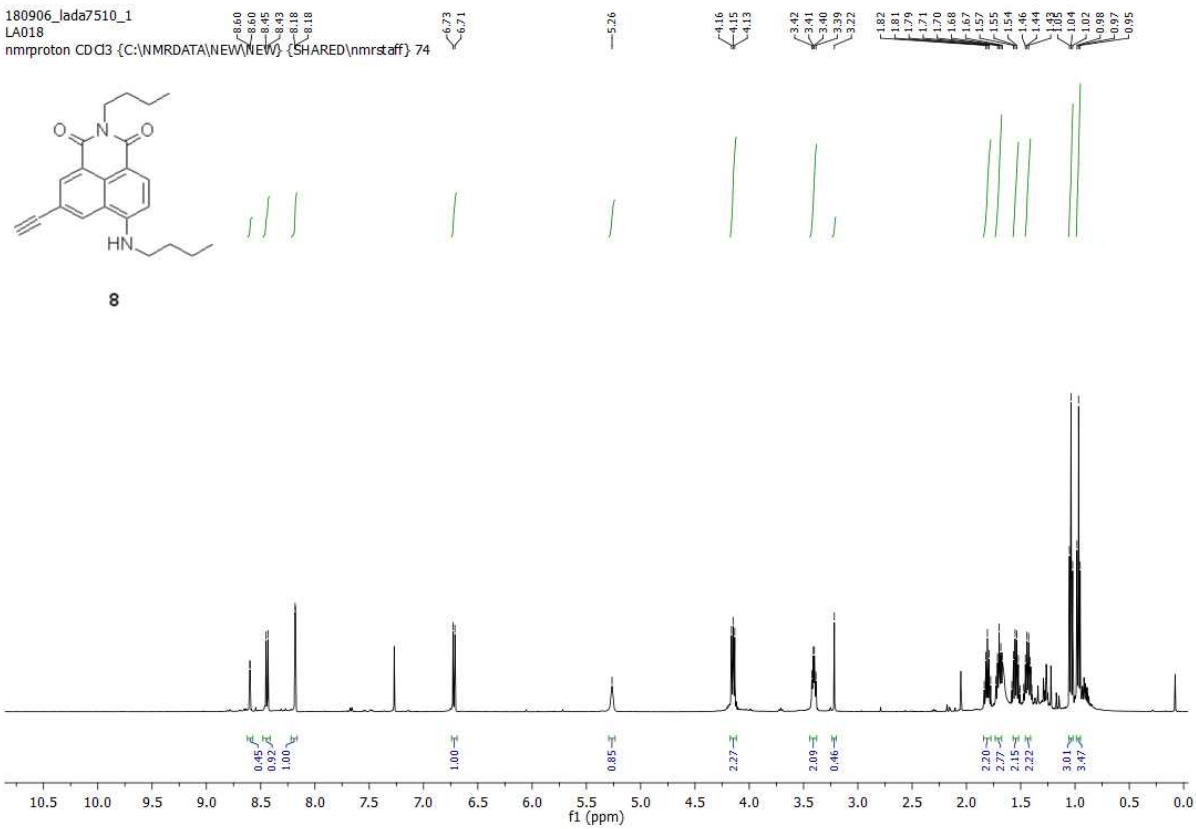
180906_lada7510_1
LA018
nmrproton CDCl3 {C:\NMRDATA\NEW\NEW} {SHARED\nmrstaff} 74
8.60
8.60
8.45
8.43
8.18
8.18
6.73
6.71
5.26
4.16
4.15
4.13
3.42
3.41
3.40
3.39
3.22
1.82
1.81
1.79
1.71
1.70
1.68
1.67
1.57
1.55
1.54
1.46
1.44
1.04
1.02
0.98
0.97
0.95
O
N
O
HN
8
0.45
0.92
1.00
1.00
0.85
2.27
2.09
0.46
2.20
2.77
2.15
2.22
3.01
3.47
10.5
10.0
9.5
9.0
8.5
8.0
7.5
7.0
6.5
6.0
5.5
5.0
4.5
4.0
3.5
3.0
2.5
2.0
1.5
1.0
0.5
0.0
f1 (ppm)

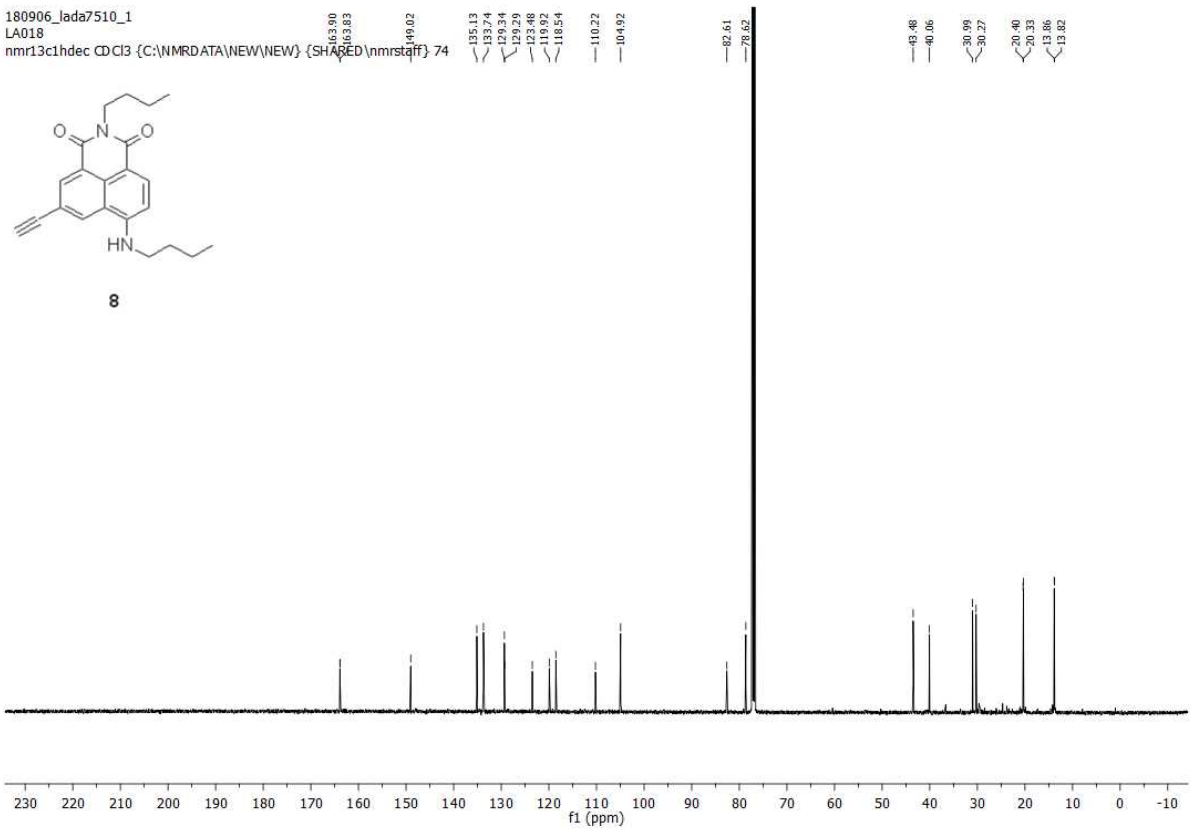
180906_lada7510_1
LA018
nmr13c1hdec CDCl3 {C:\NMRDATA\NEW\NEW} {SHARED\nmrstaff} 74
163.90
163.83
149.02
135.13
133.74
129.34
129.29
123.48
119.92
118.54
110.22
104.92
82.61
78.62
43.48
40.06
30.99
30.27
20.40
20.33
13.86
13.82
O
N
O
HN
8
230
220
210
200
190
180
170
160
150
140
130
120
110
100
90
80
70
60
50
40
30
20
10
0
-10
f1 (ppm)

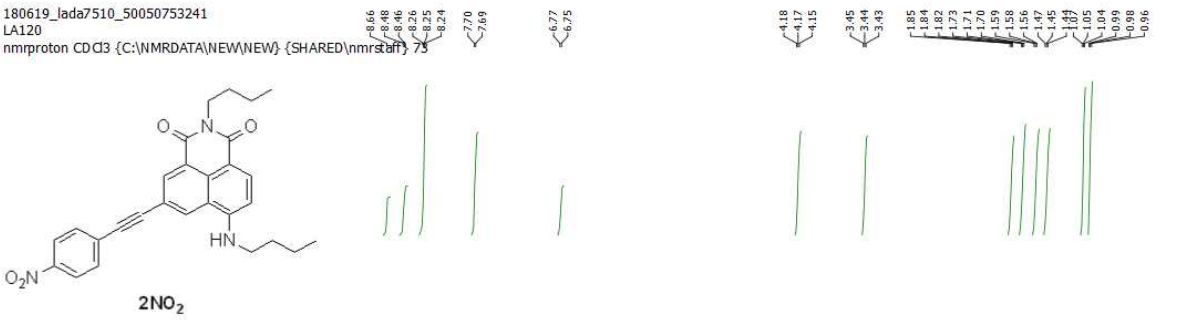
180619_lada7510_50050753241
LA120
nmrproton CDCl3 {C:\NMRDATA\NEW\NEW} {SHARED\nmrstaff} 73
8.66
8.48
8.46
8.26
8.25
8.24
7.70
7.69
6.77
6.75
4.18
4.17
4.15
3.45
3.44
3.43
1.85
1.84
1.82
1.73
1.71
1.70
1.59
1.58
1.56
1.47
1.45
1.44
1.07
1.05
1.04
0.99
0.98
0.96

O
N
O
HN
O2N

2NO$_2$

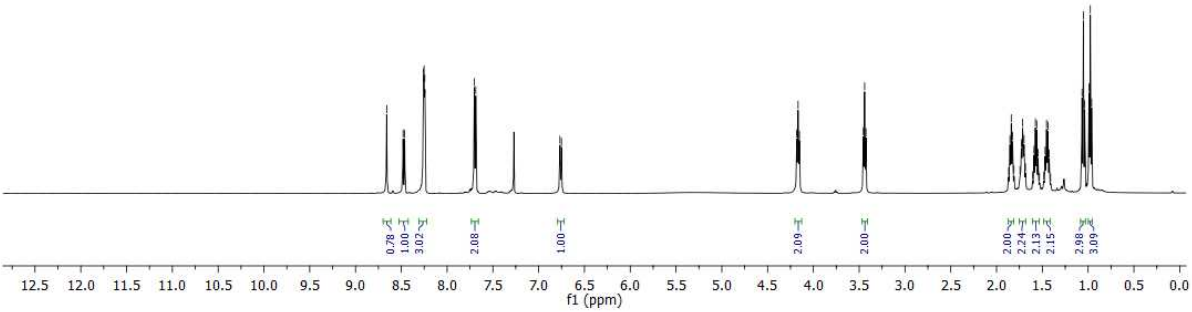
0.78
1.00
3.02
2.08
1.00
2.09
2.00
2.00
2.24
2.13
2.15
2.98
3.09
12.5 12.0 11.5 11.0 10.5 10.0 9.5 9.0 8.5 8.0 7.5 7.0 6.5 6.0 5.5 5.0 4.5 4.0 3.5 3.0 2.5 2.0 1.5 1.0 0.5 0.0
f1 (ppm)

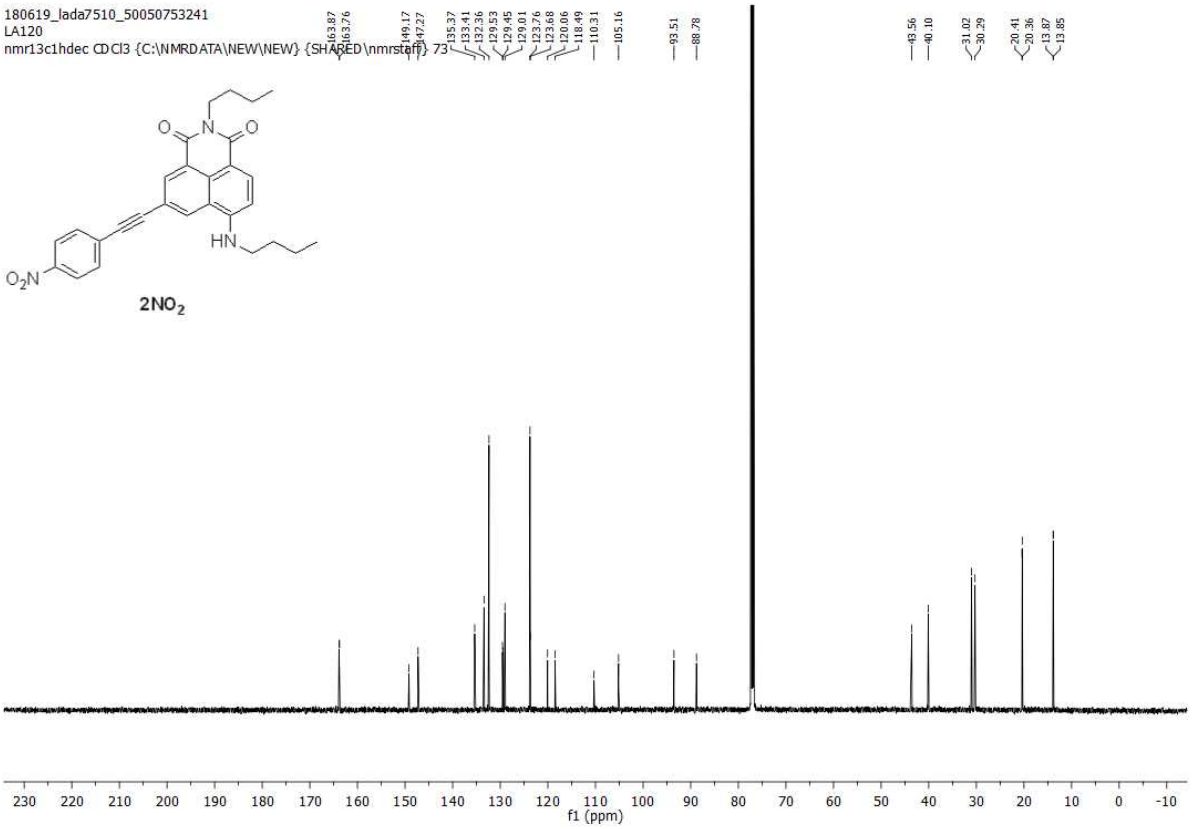
180619_lada7510_50050753241
LA120
nmr13c1hdec CDCl3 {C:\NMRDATA\NEW\NEW} {SHARED\nmrstaff} 73
163.87
163.76
149.17
147.27
135.37
133.41
132.36
129.53
129.45
129.01
123.76
123.68
120.06
118.49
110.31
105.16
93.51
88.78
43.56
40.10
31.02
30.29
20.41
20.36
13.87
13.85
230 220 210 200 190 180 170 160 150 140 130 120 110 100 90 80 70 60 50 40 30 20 10 0 -10
f1 (ppm)

O
N
O
HN
O2N

2NO$_2$

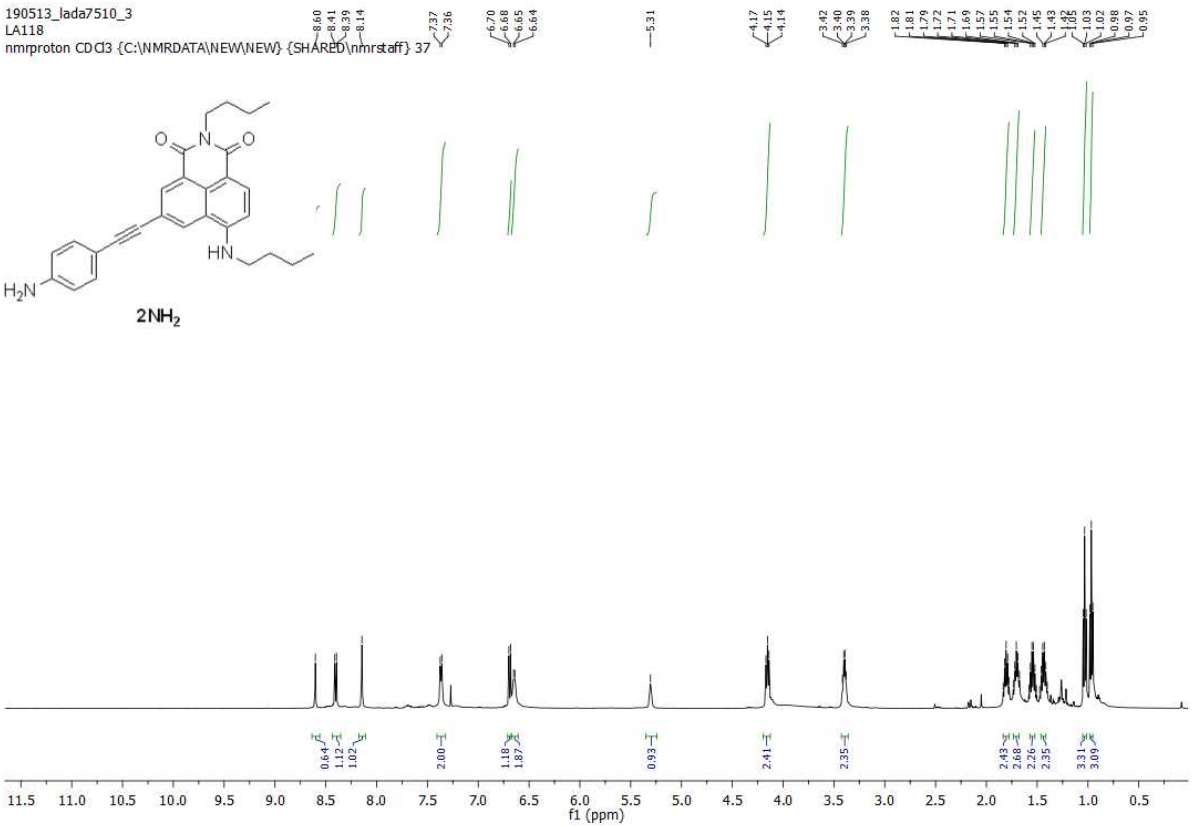
190513_lada7510_3
LA118
nmrproton CDCl3 {C:\NMRDATA\NEW\NEW} {SHARED\nmrstaff} 37
8.60
8.41
8.39
8.14
7.37
7.36
6.70
6.68
6.65
6.64
5.31
4.17
4.15
4.14
3.42
3.40
3.39
3.38
1.82
1.81
1.79
1.72
1.71
1.69
1.57
1.55
1.54
1.52
1.45
1.43
1.03
1.02
0.98
0.97
0.95
O
N
O
HN
H2N
2NH2
0.64
1.12
1.02
2.00
1.18
1.87
0.93
2.41
2.35
2.43
2.68
2.26
2.35
3.31
3.09
11.5 11.0 10.5 10.0 9.5 9.0 8.5 8.0 7.5 7.0 6.5 6.0 5.5 5.0 4.5 4.0 3.5 3.0 2.5 2.0 1.5 1.0 0.5
f1 (ppm)

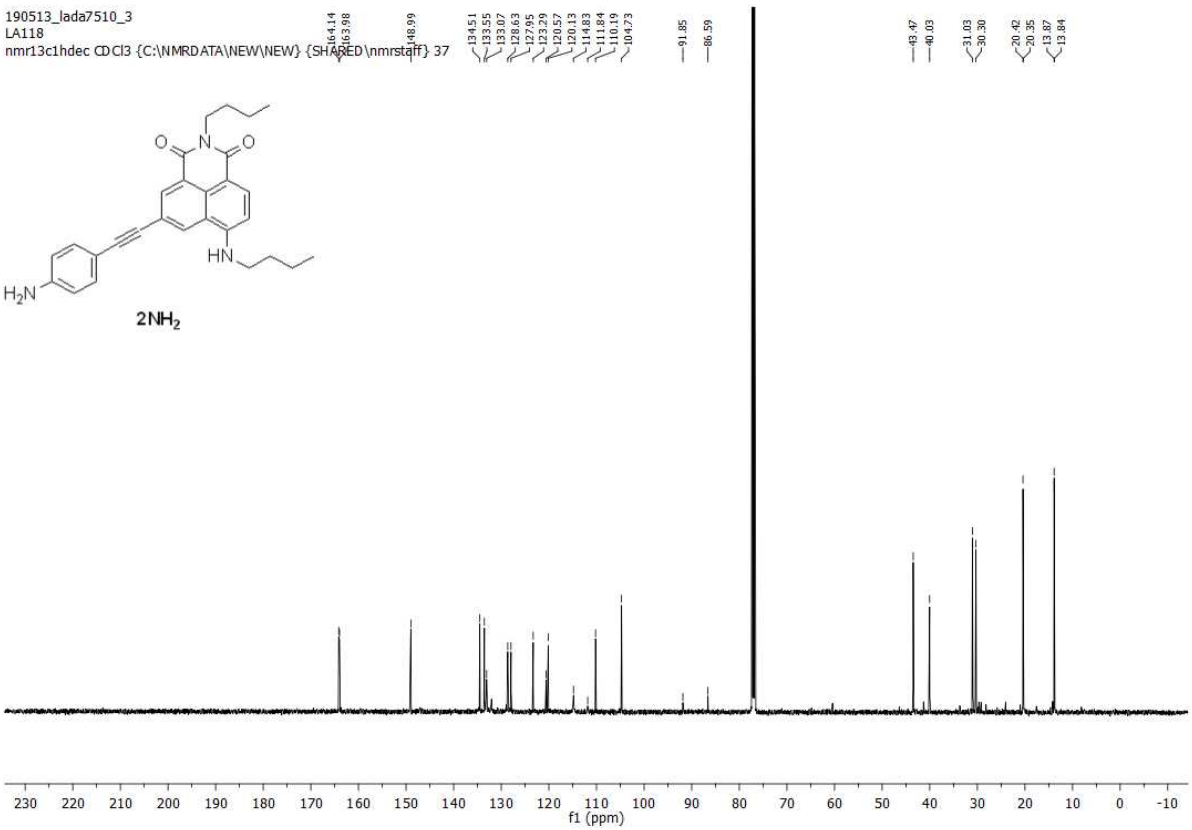
190513_lada7510_3
LA118
nmr13c1hdec CDCl3 {C:\NMRDATA\NEW\NEW} {SHARED\nmrstaff} 37
164.14
163.98
148.99
134.51
133.55
133.07
128.63
127.95
122.29
120.57
120.13
114.83
111.84
110.19
104.73
91.85
86.59
43.47
40.03
31.03
30.30
20.42
20.35
13.87
13.84
O
N
O
HN
H2N
2NH2
230 220 210 200 190 180 170 160 150 140 130 120 110 100 90 80 70 60 50 40 30 20 10 0 -10
f1 (ppm)

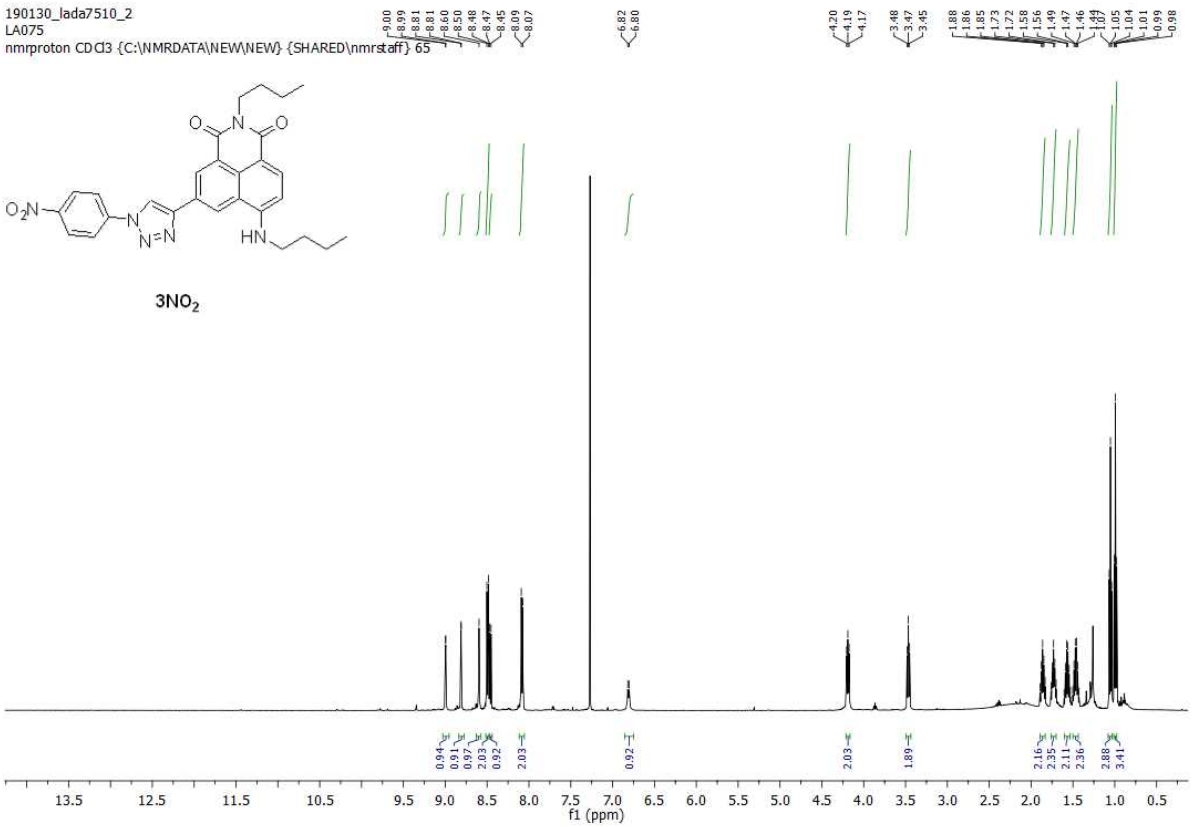
190130_lada7510_2
LA075
nmrproton CDCl3 {C:\NMRDATA\NEW\NEW} {SHARED\nmrstaff} 65
9.00
8.99
8.81
8.81
8.60
8.50
8.48
8.47
8.45
8.09
8.07
6.82
6.80
4.20
4.19
4.17
3.48
3.47
3.45
1.88
1.86
1.85
1.73
1.72
1.58
1.56
1.49
1.47
1.46
1.05
1.04
1.01
0.99
0.98
O2N
N
N=N
O
N
O
HN
3NO2
0.94
0.91
0.97
2.03
0.92
2.03
0.92
2.03
1.89
2.16
2.35
2.11
2.36
2.88
3.41
13.5
12.5
11.5
10.5
9.5
9.0
8.5
8.0
7.5
7.0
6.5
6.0
5.5
5.0
4.5
4.0
3.5
3.0
2.5
2.0
1.5
1.0
0.5
f1 (ppm)

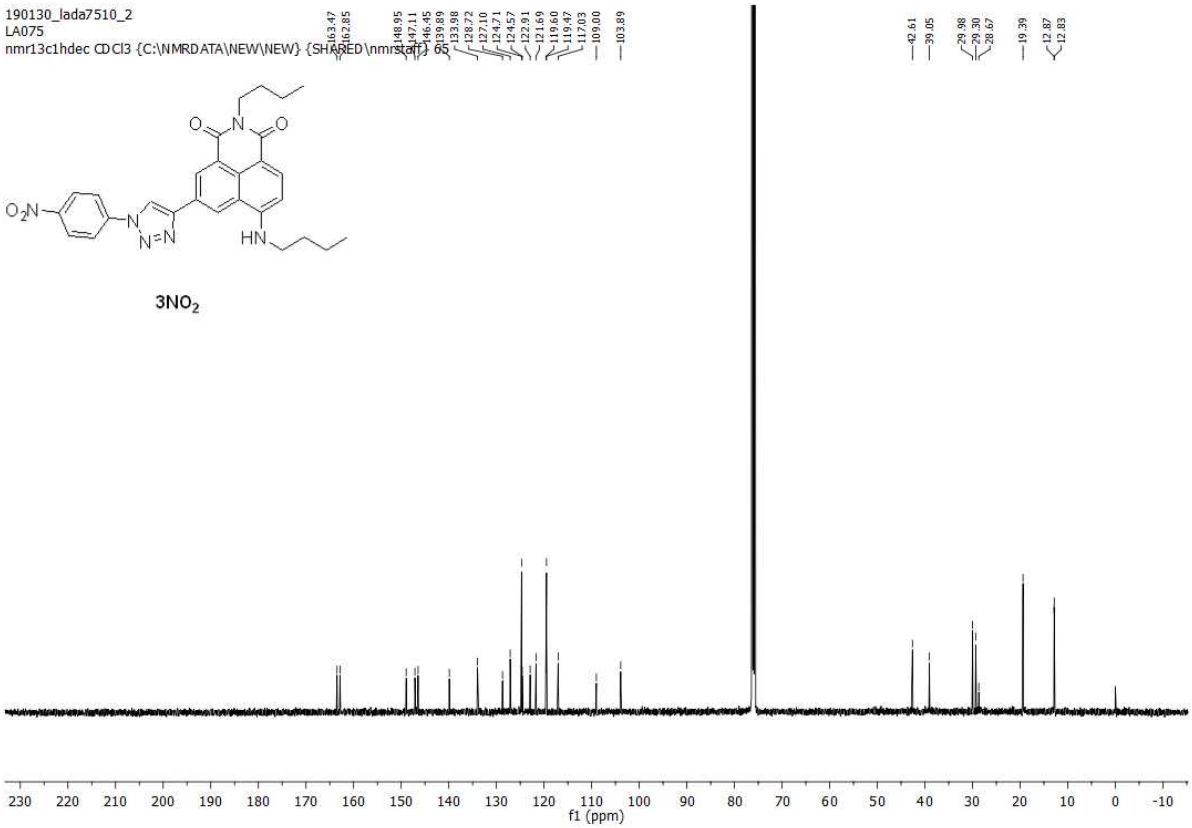
190130_lada7510_2
LA075
nmr13c1hdec CDCl3 {C:\NMRDATA\NEW\NEW} {SHARED\nmrstaff} 65
163.47
162.85
148.95
147.11
146.45
139.89
133.98
128.72
127.10
124.71
124.57
122.91
121.69
119.60
119.47
117.03
109.00
103.89
42.61
39.05
29.98
29.30
28.67
19.39
12.87
12.83
O2N
N
N=N
O
N
O
HN
3NO2
230
220
210
200
190
180
170
160
150
140
130
120
110
100
90
80
70
60
50
40
30
20
10
0
-10
f1 (ppm)

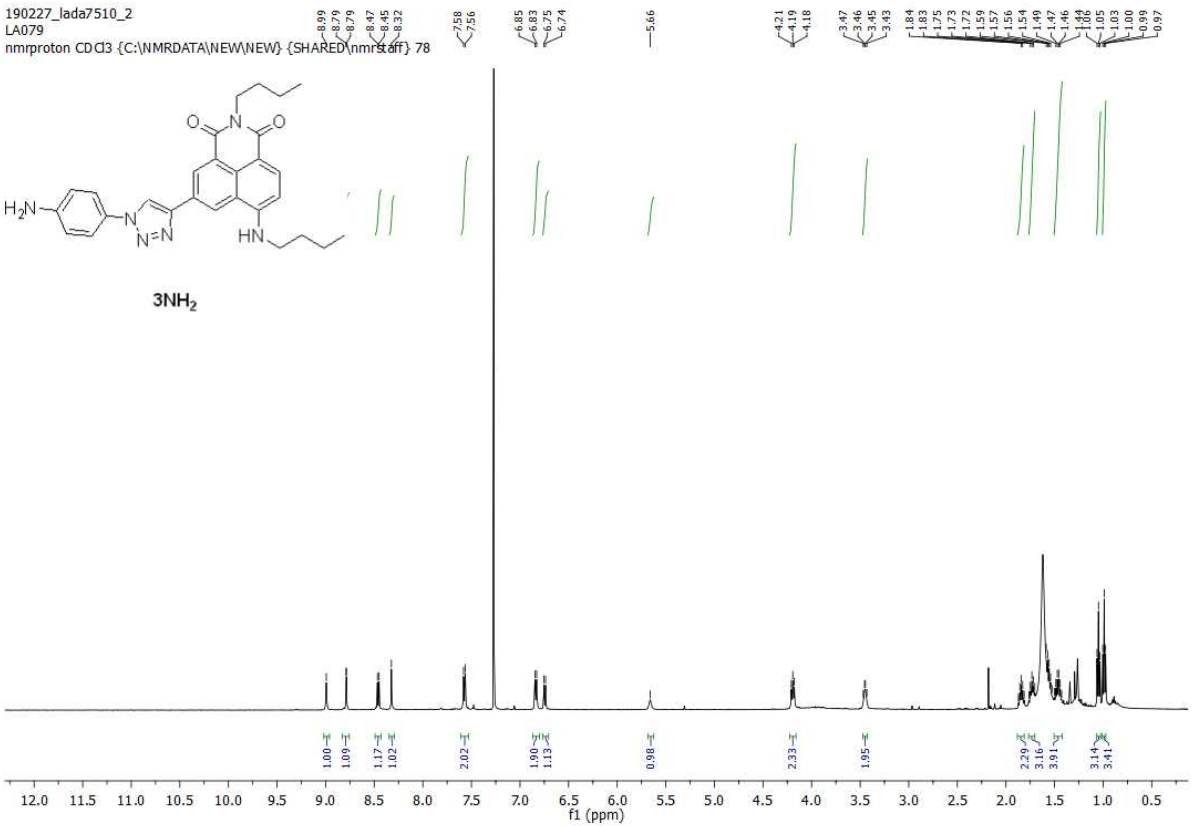
190227_lada7510_2
LA079
nmrproton CDCl3 {C:\NMRDATA\NEW\NEW} {SHARED\nmrstaff} 78
3NH2
f1 (ppm)

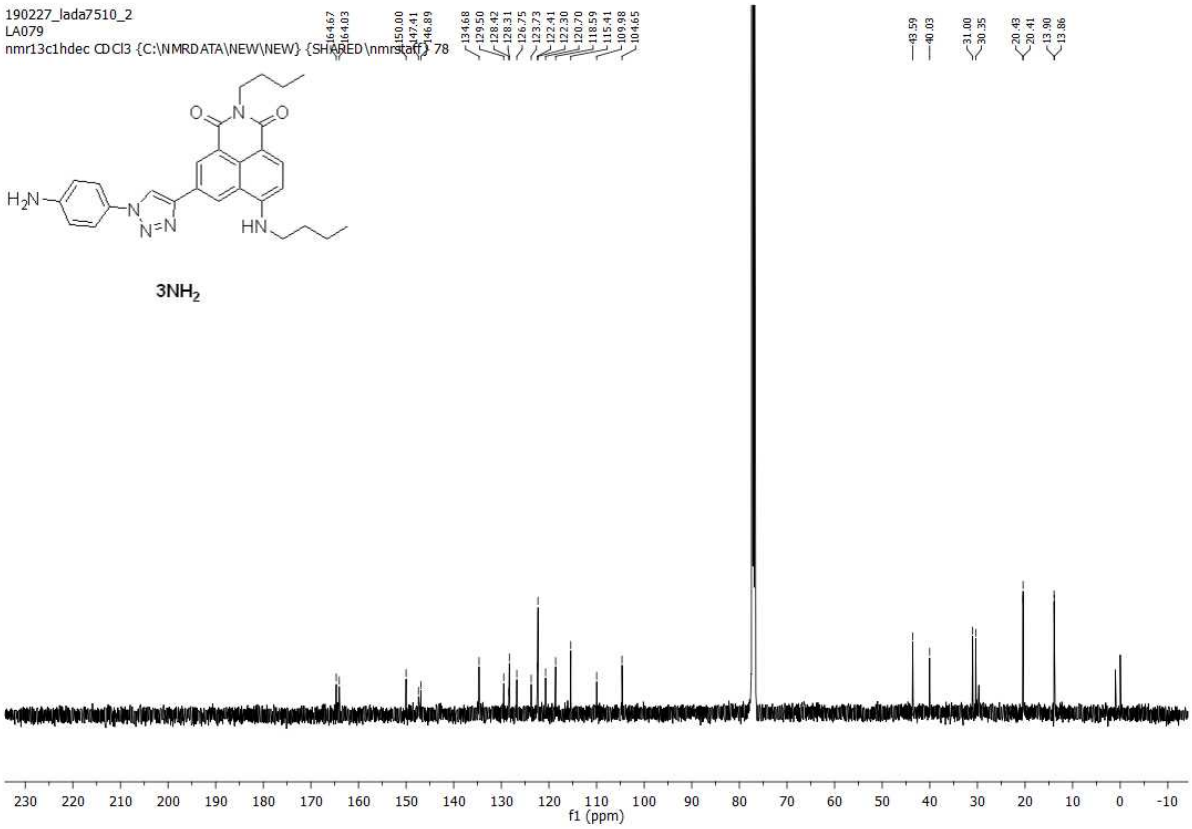
190227_lada7510_2
LA079
nmr13c1hdec CDCl3 {C:\NMRDATA\NEW\NEW} {SHARED\nmrstaff} 78
3NH2
f1 (ppm)

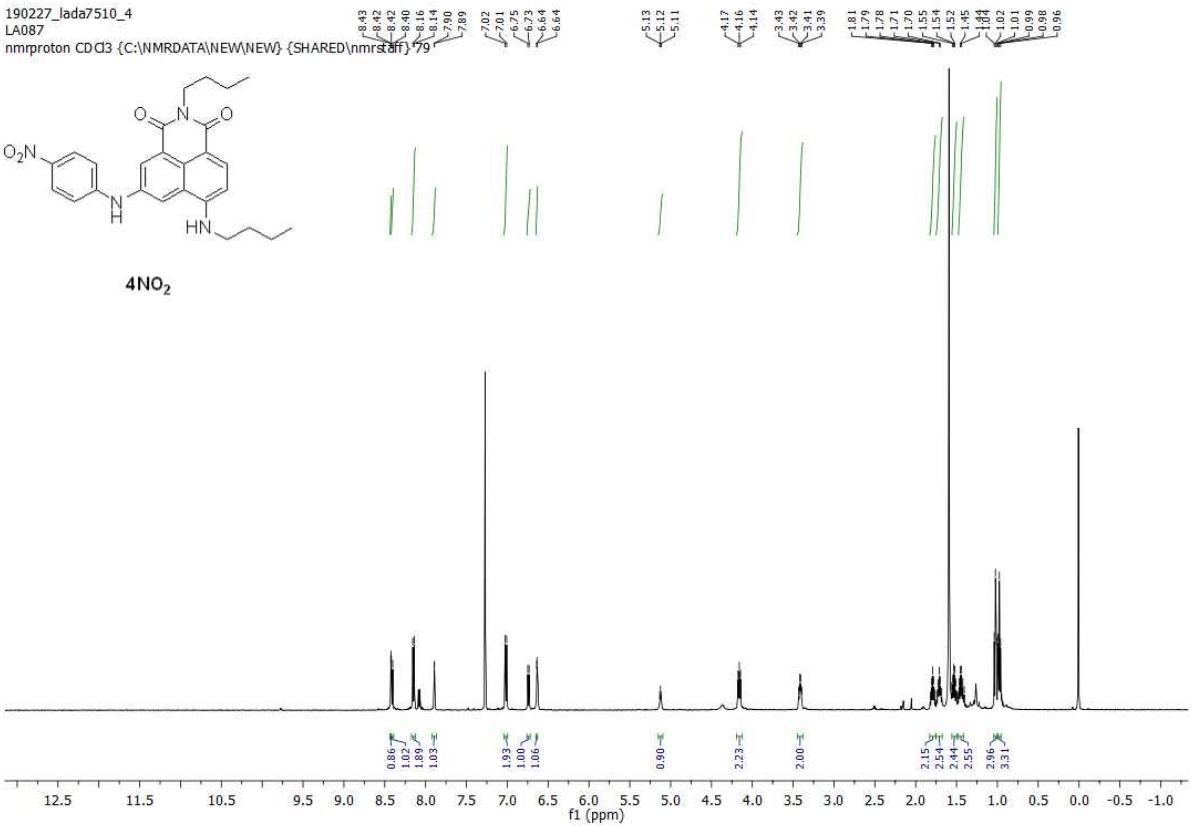
190227_lada7510_4
LA087
nmrproton CDCl3 {C:\NMRDATA\NEW\NEW} {SHARED\nmrstaff} 79
8.43
8.42
8.42
8.40
8.16
8.14
7.90
7.89
7.02
7.01
6.75
6.73
6.64
6.64
5.13
5.12
5.11
4.17
4.16
4.14
3.43
3.42
3.41
3.39
1.81
1.79
1.78
1.71
1.70
1.55
1.54
1.52
1.45
1.44
1.02
1.01
0.99
0.98
0.96
O2N
N
H
HN
O
N
O
4NO2
0.86
1.02
1.89
1.03
1.93
1.00
1.06
0.90
2.23
2.00
2.15
2.54
2.44
2.55
2.96
3.31
12.5
11.5
10.5
9.5
9.0
8.5
8.0
7.5
7.0
6.5
6.0
5.5
5.0
4.5
4.0
3.5
3.0
2.5
2.0
1.5
1.0
0.5
0.0
-0.5
-1.0
f1 (ppm)

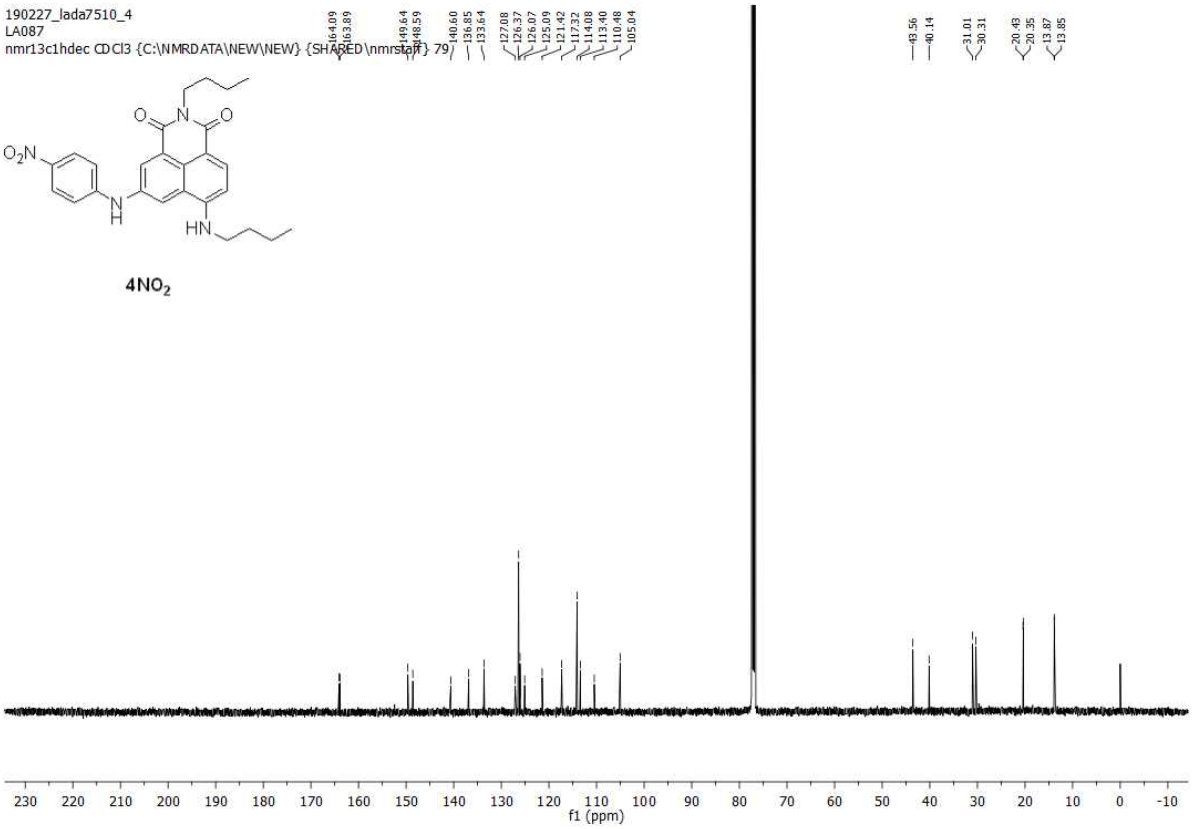
190227_lada7510_4
LA087
nmr13c1hdec CDCl3 {C:\NMRDATA\NEW\NEW} {SHARED\nmrstaff} 79
164.09
163.89
149.64
148.59
140.60
136.85
133.64
127.08
126.37
126.07
125.09
121.42
117.32
114.08
113.40
110.48
105.04
43.56
40.14
31.01
30.31
20.43
20.35
13.87
13.85
O2N
N
H
HN
O
N
O
4NO2
230
220
210
200
190
180
170
160
150
140
130
120
110
100
90
80
70
60
50
40
30
20
10
0
-10
f1 (ppm)

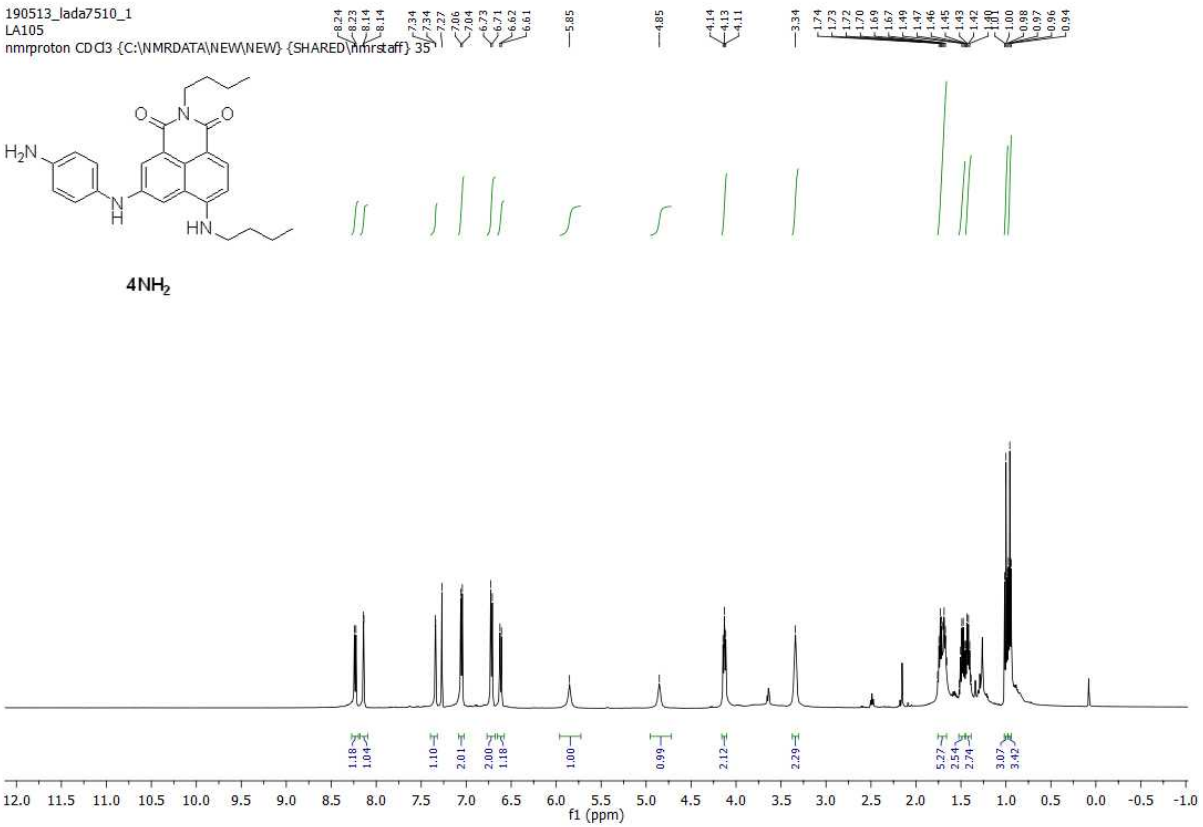
190513_lada7510_1
LA105
nmrproton CDCl3 {C:\NMRDATA\NEW\NEW} {SHARED\nmrstaff} 35
8.24
8.23
8.14
8.14
7.34
7.34
7.27
7.06
7.04
6.73
6.71
6.62
6.61
5.85
4.85
4.14
4.13
4.11
3.34
1.74
1.73
1.72
1.70
1.69
1.67
1.49
1.47
1.46
1.45
1.43
1.42
1.01
1.00
0.98
0.97
0.96
0.94
1.18
1.04
1.10
2.01
2.00
1.18
1.00
0.99
2.12
2.29
5.27
2.54
2.74
3.07
3.42
f1 (ppm)

4NH$_2$

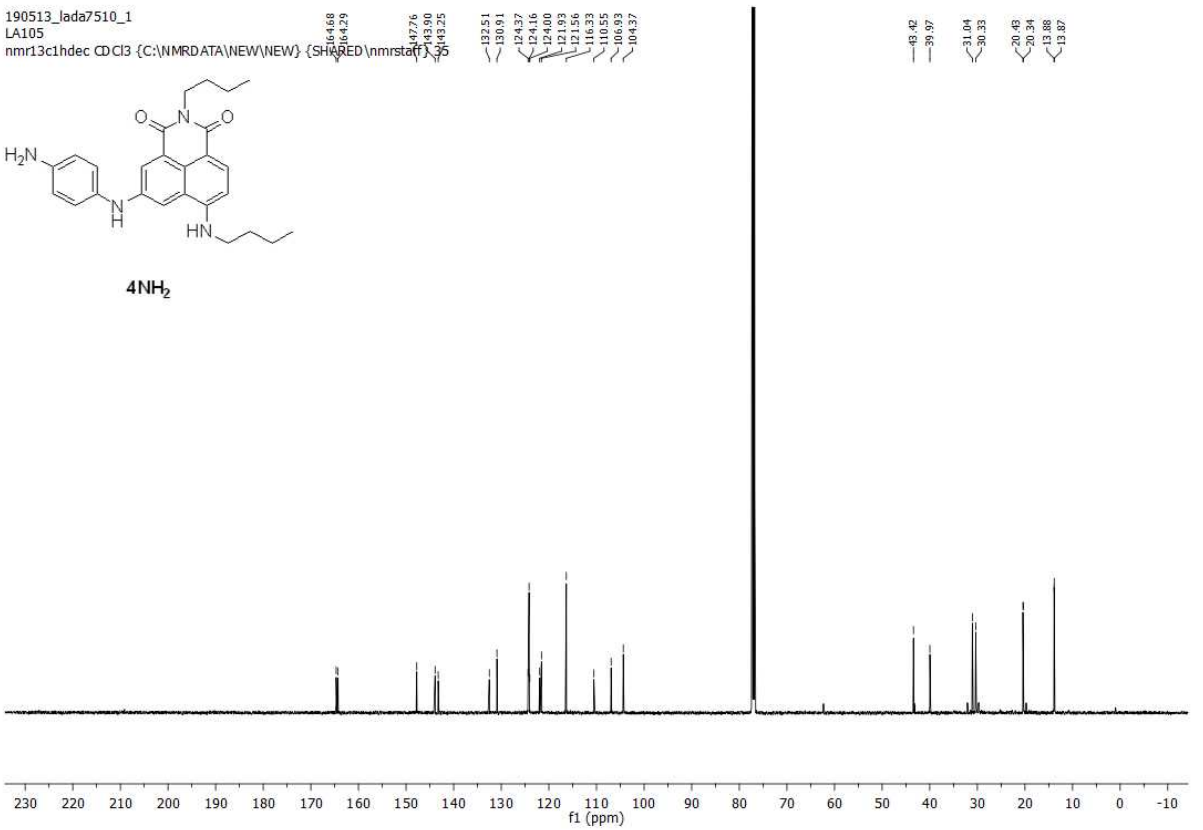
190513_lada7510_1
LA105
nmr13c1hdec CDCl3 {C:\NMRDATA\NEW\NEW} {SHARED\nmrstaff} 35
164.68
164.29
147.76
143.90
143.25
132.51
130.91
124.37
124.16
124.00
121.93
121.56
116.33
110.55
106.93
104.37
43.42
39.97
31.04
30.33
20.43
20.34
13.88
13.87
f1 (ppm)

4NH$_2$

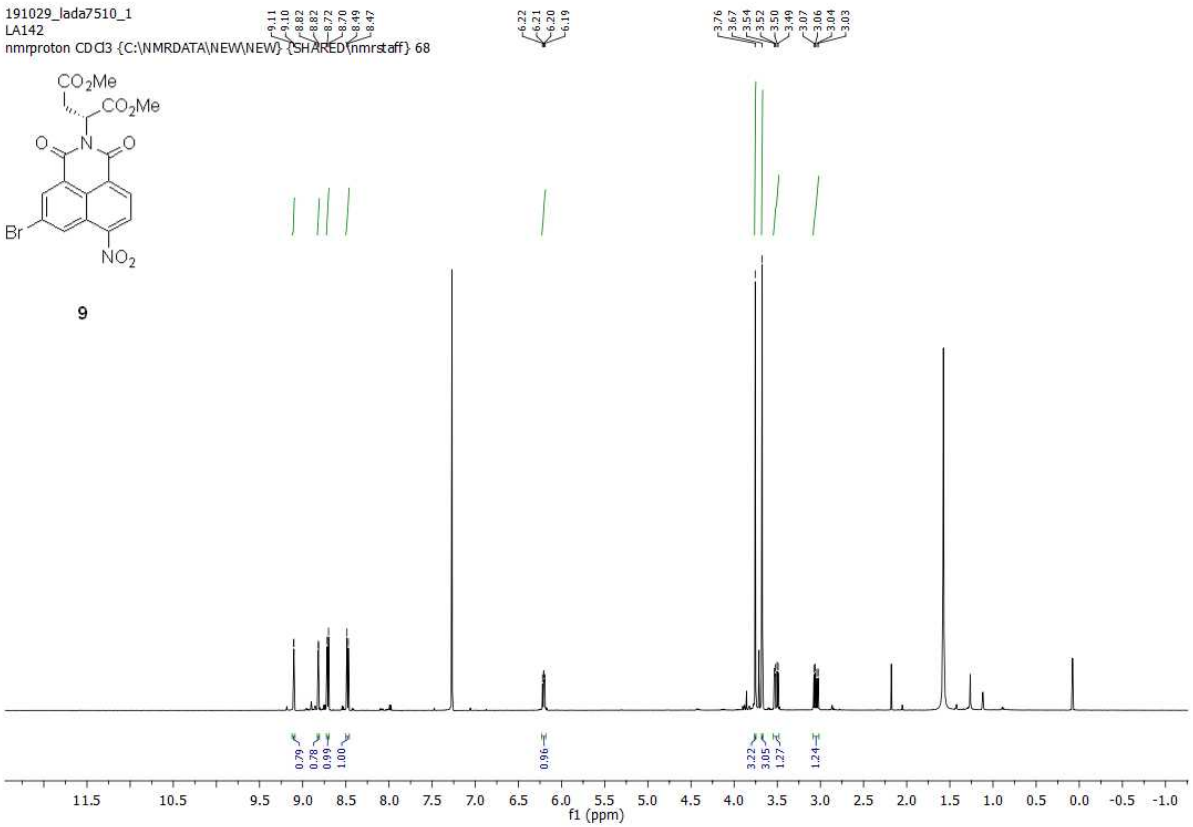
191029_lada7510_1
LA142
nmrproton CDCl3 {C:\NMRDATA\NEW\NEW} {SHARED\nmrstaff} 68
9.11
9.10
8.82
8.82
8.72
8.70
8.49
8.47
6.22
6.21
6.20
6.19
3.76
3.67
3.54
3.52
3.50
3.49
3.07
3.06
3.04
3.03
CO2Me
CO2Me
O
N
O
Br
NO2
9
0.79
0.78
0.99
1.00
0.96
3.22
3.05
1.27
1.24
11.5
10.5
9.5
9.0
8.5
8.0
7.5
7.0
6.5
6.0
5.5
5.0
4.5
4.0
3.5
3.0
2.5
2.0
1.5
1.0
0.5
0.0
-0.5
-1.0
f1 (ppm)

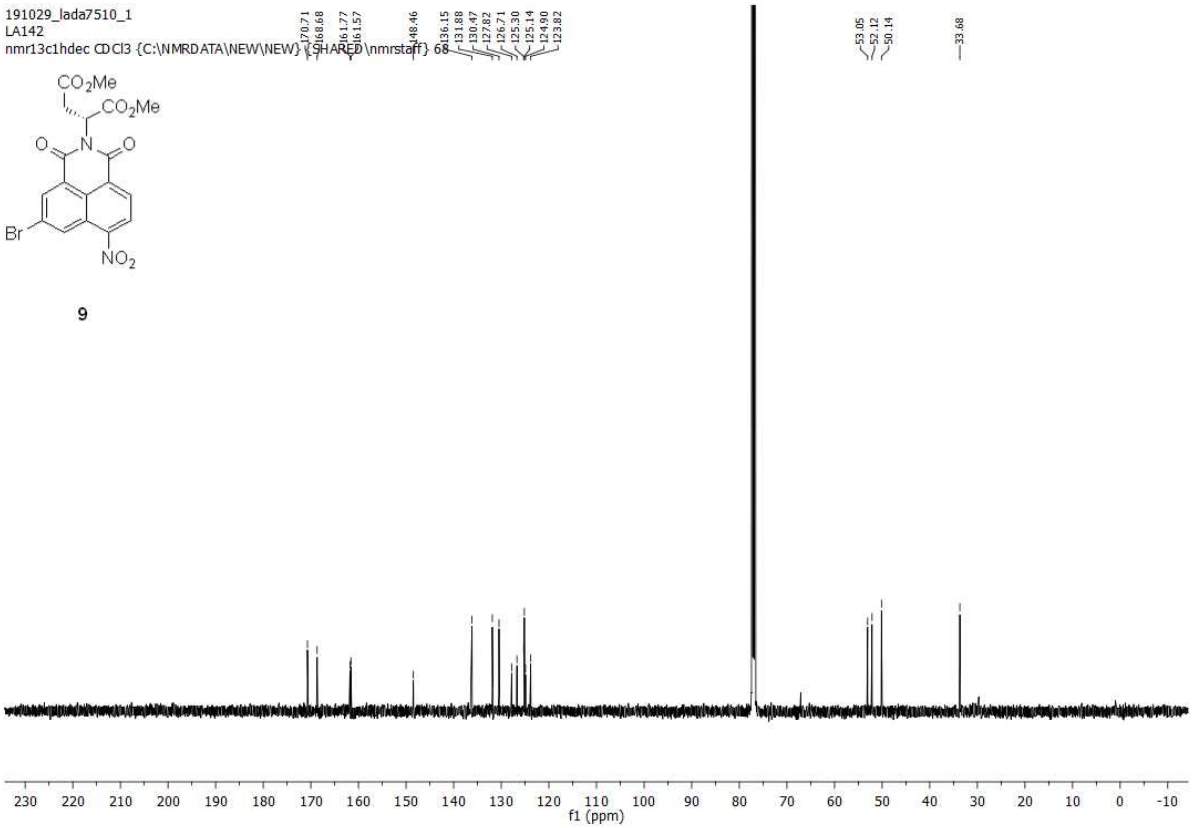
191029_lada7510_1
LA142
nmr13c1hdec CDCl3 {C:\NMRDATA\NEW\NEW} {SHARED\nmrstaff} 68
170.71
168.68
161.77
161.57
148.46
136.15
131.88
130.47
127.82
126.71
125.30
125.14
124.90
123.82
53.05
52.12
50.14
33.68
CO2Me
CO2Me
O
N
O
Br
NO2
9
230
220
210
200
190
180
170
160
150
140
130
120
110
100
90
80
70
60
50
40
30
20
10
0
-10
f1 (ppm)

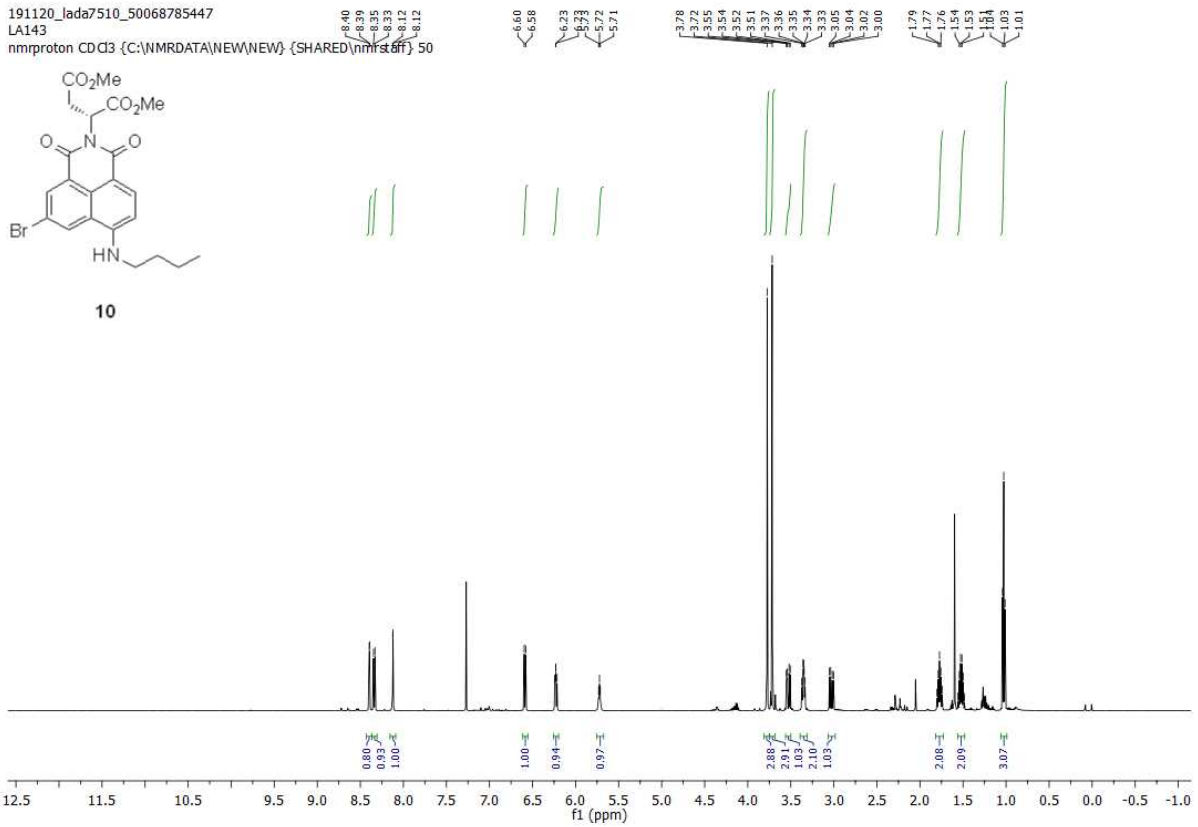
191120_lada7510_50068785447
LA143
nmrproton CDCl3 {C:\NMRDATA\NEW\NEW} {SHARED\nmrstaff} 50
10
f1 (ppm)

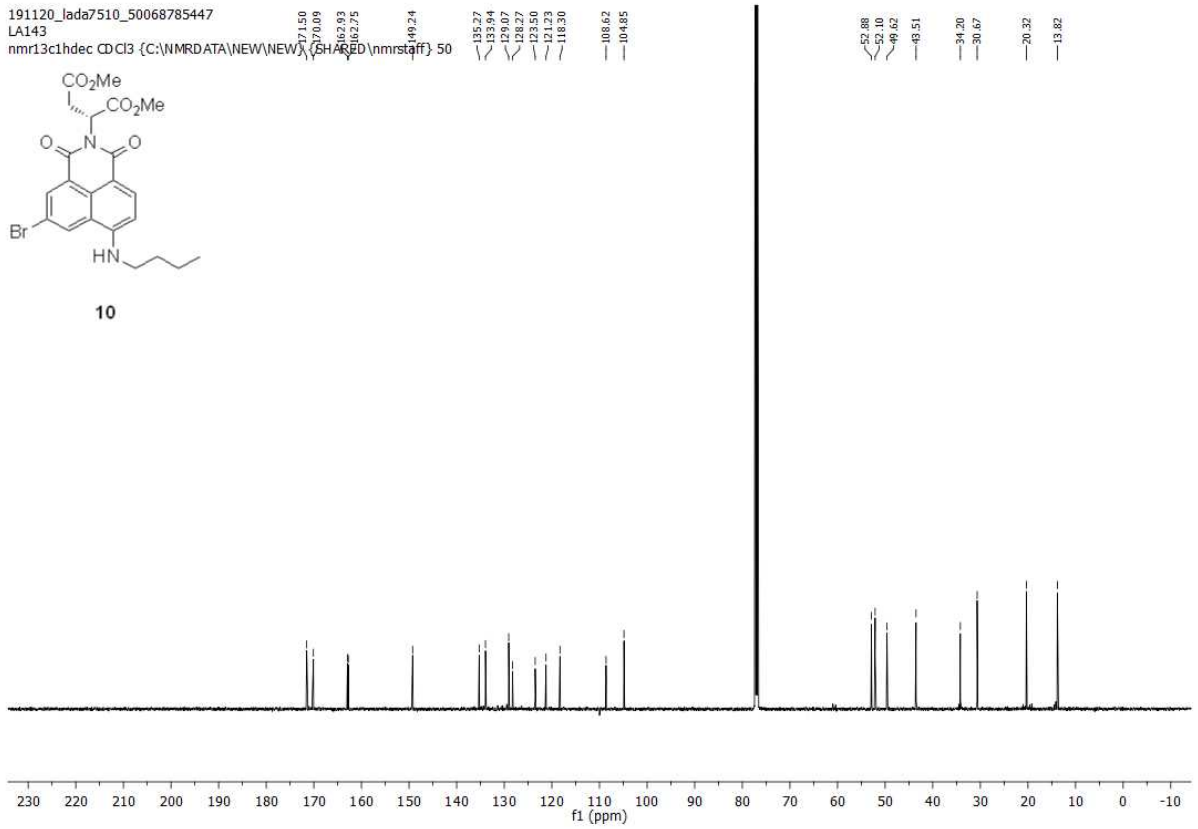
191120_lada7510_50068785447
LA143
nmr13c1hdec CDCl3 {C:\NMRDATA\NEW\NEW} {SHARED\nmrstaff} 50
10
f1 (ppm)

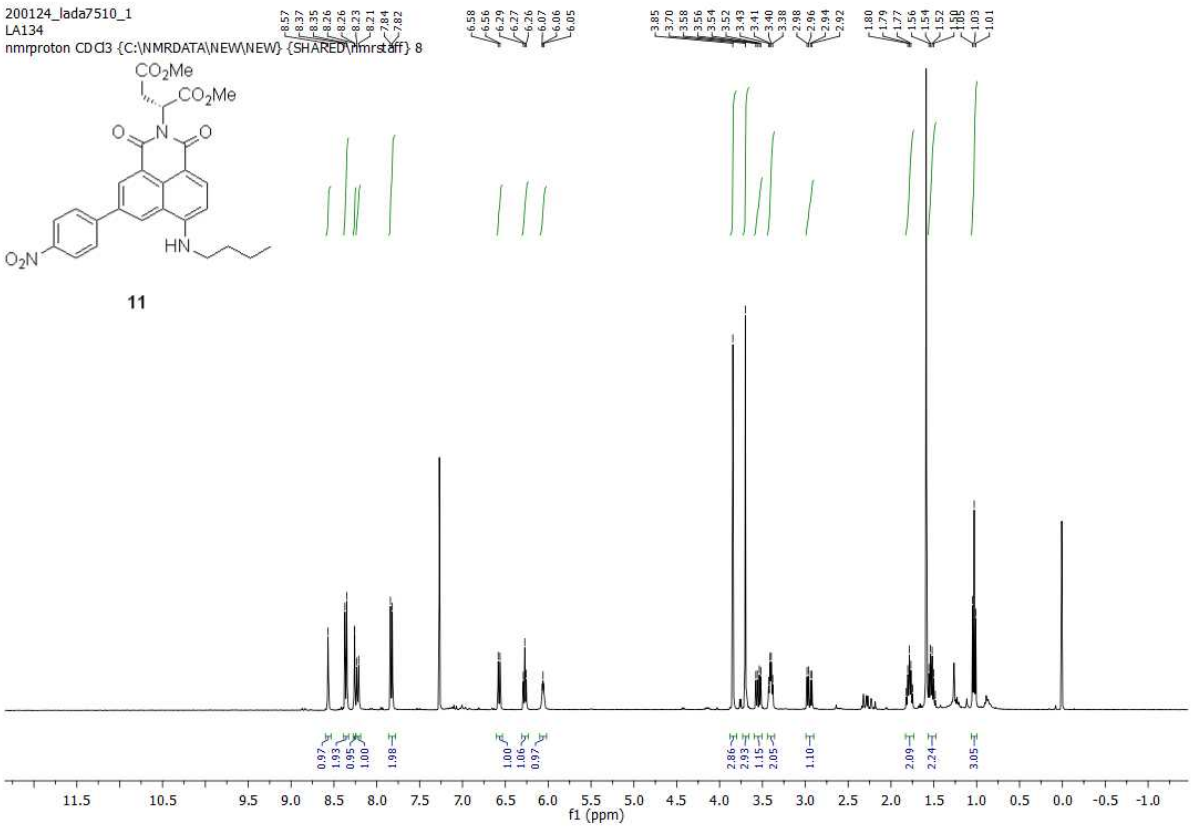
200124_lada7510_1
LA134
nmrproton CDCl3 {C:\NMRDATA\NEW\NEW} {SHARED\nmrstaff} 8
11
f1 (ppm)

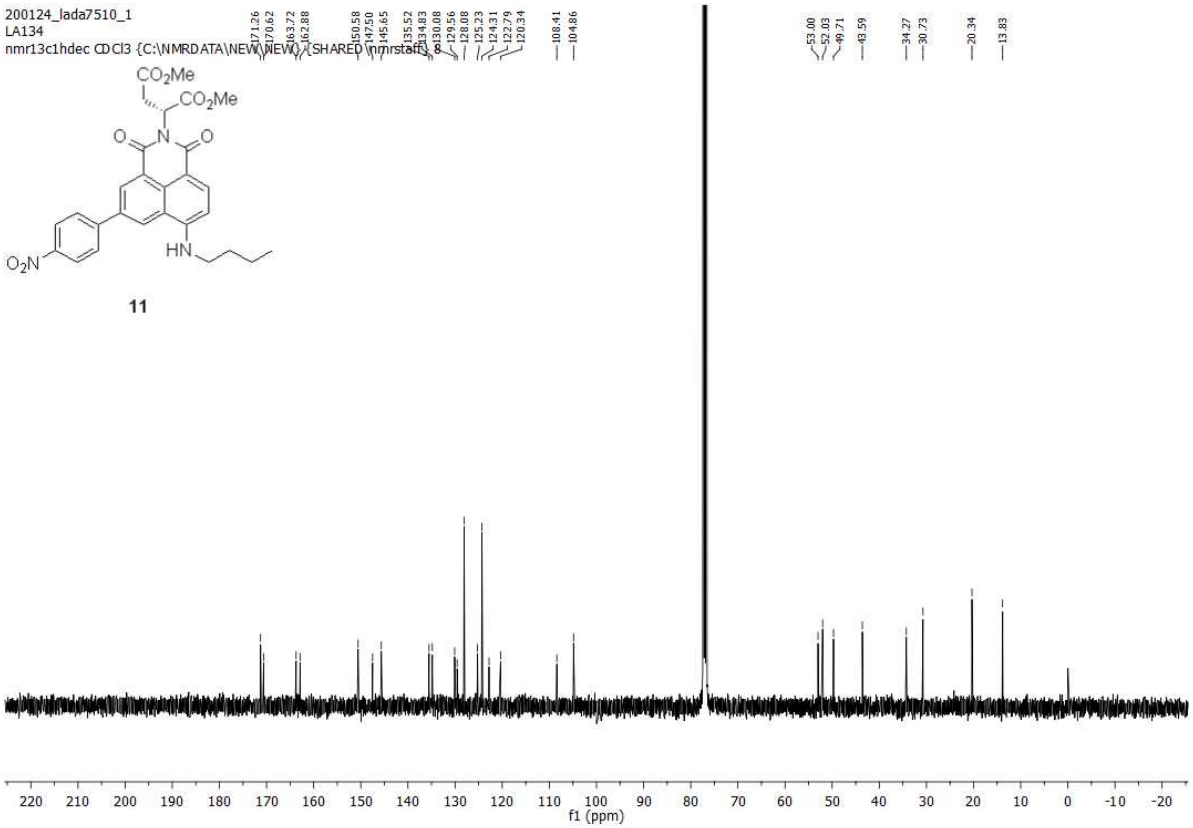
200124_lada7510_1
LA134
nmr13c1hdec CDCl3 {C:\NMRDATA\NEW\NEW} {SHARED\nmrstaff} 8
11
f1 (ppm)

LA138 040220
LA138

Asp-1NO$_2$

200208_lada7510_1

Asp-1NO$_2$

References

[1] K. G. Leslie, D. Jacquemin, E. J. New, K. A. Jolliffe, *Chem-Eur J* **2018**, *24*, 5569-5573.

[2] K. D. Grimes, A. Gupte, C. C. Aldrich, *Synthesis-Stuttgart* **2010**, 1441-1448.

[3] K. Omata, S. Aoyagi, K. Kabuto, *Tetrahedron: Asymmetry* **2004**, *15*, 2351-2356.

[4] *Vol. V6.2*, TURBOMOLE V6.2 2010, A development of University of Karlsruhe and Forschungszentrum Karlsruhe GmbH, 1989 - 2007, Turbomole GmbH available from https://www.turbomole.org.

[5] M. J. Frisch, G. W. Trucks, H. B. Schlegel, G. E. Scuseria, M. A. Robb, J. R. Cheeseman, G. Scalmani, V. Barone, G. A. Petersson, H. Nakatsuji, X. Li, M. Caricato, A. V. Marenich, J. Bloino, B. G. Janesko, R. Gomperts, B. Mennucci, H. P. Hratchian, J. V. Ortiz, A. F. Izmaylov, J. L. Sonnenberg, Williams, F. Ding, F. Lipparini, F. Egidi, J. Goings, B. Peng, A. Petrone, T. Henderson, D. Ranasinghe, V. G. Zakrzewski, J. Gao, N. Rega, G. Zheng, W. Liang, M. Hada, M. Ehara, K. Toyota, R. Fukuda, J. Hasegawa, M. Ishida, T. Nakajima, Y. Honda, O. Kitao, H. Nakai, T. Vreven, K. Throssell, J. A. Montgomery Jr., J. E. Peralta, F. Ogliaro, M. J. Bearpark, J. J. Heyd, E. N. Brothers, K. N. Kudin, V. N. Staroverov, T. A. Keith, R. Kobayashi, J. Normand, K. Raghavachari, A. P. Rendell, J. C. Burant, S. S. Iyengar, J. Tomasi, M. Cossi, J. M. Millam, M. Klene, C. Adamo, R. Cammi, J. W. Ochterski, R. L. Martin, K. Morokuma, O. Farkas, J. B. Foresman, D. J. Fox, Wallingford, CT, **2016**.

[6] Y. Zhao, D. G. Truhlar, *Theoretical Chemistry Accounts* **2008**, *120*, 215-241.

[7] B. Le Guennic, D. Jacquemin, *Accounts of Chemical Research* **2015**, *48*, 530-537.

[8] J. Tomasi, B. Mennucci, R. Cammi, *Chemical Reviews* **2005**, *105*, 2999-3094.

[9] a) P. M. Vérité, C. A. Guido, D. Jacquemin, *Physical Chemistry Chemical Physics* **2019**, *21*, 2307-2317; b) M. Caricato, B. Mennucci, J. Tomasi, F. Ingrosso, R. Cammi, S. Corni, G. Scalmani, *The Journal of Chemical Physics* **2006**, *124*, 124520.